

# Geochemical characterization of the Nirano Mud Volcano, Italy

Alessandra Sciarra<sup>(a,d,e)\*</sup>, Barbara Cantucci<sup>(a)</sup>, Tullio Ricci<sup>(a)</sup>, Yama Tomonaga<sup>(b,f)</sup>, Adriano Mazzini<sup>(c)</sup>

<sup>(a)</sup> Istituto Nazionale di Geofisica e Vulcanologia, Rome, Italy ([alessandra.sciarra@ingv.it](mailto:alessandra.sciarra@ingv.it)),

<sup>(b)</sup> Institute of Geological Sciences, University of Bern, Switzerland

<sup>(c)</sup> Centre for Earth Evolution and Dynamics, University of Oslo, Norway

<sup>(d)</sup> CNR-IGAG, Consiglio Nazionale delle Ricerche- Istituto di Geologia Ambientale e Geoingegneria, Rome, Italy

<sup>(e)</sup> University of Ferrara, Department of Physics and Earth Sciences, Ferrara, Italy

<sup>(f)</sup> Eawag, Swiss Federal Institute of Aquatic Science and Technology, Dübendorf, Switzerland

\*Corresponding author: Alessandra Sciarra ([alessandra.sciarra@ingv.it](mailto:alessandra.sciarra@ingv.it))

## Abstract

The Nirano mud volcano is located in the western sector of the Modena Apennine margin (Italy). It represents one of the most spectacular phenomena of sedimentary volcanism in the entire Italian territory and is among the largest in Europe. Here numerous aligned gryphon clusters and seeping pools constantly burst gas and mud resulting inside a morphological depression. Besides the obvious surface expressions of these emission spots, until now the type and amount of gas released in the rest of the large Nirano caldera zone remained unknown.

An extensive geochemical soil gas survey ( $O_2$ ,  $N_2$ ,  $CO_2$ ,  $CH_4$ ,  $^{222}Rn$ , He,  $H_2$ , and light hydrocarbons) and exhalation fluxes ( $CO_2$  and  $CH_4$ ), was carried out inside the mud volcano field with the aim of identifying soil degassing distribution, and to estimate the micro- and macro-seepage budget for both  $CO_2$  and  $CH_4$ .

Soil gas data highlight the presence of two zones characterized by high concentrations and flux values. These enhanced seepage zones are located in the SW and NE sectors of the mud volcano suggesting that the enhanced gas emissions present in the peripheral zones, are controlled by caldera collapse structures. The most significant  $CO_2$  flux (up to  $91 \text{ g m}^{-2} \text{ d}^{-1}$ ) and  $^{222}Rn$  anomalies are located in the central part of the crater in correspondence of a morphological escarpment. Here we infer the presence of a buried tectonic system of collapsed terraces that facilitate fluids degassing. In contrast,  $CH_4$  fluxes show a scattered distribution and low values (mean  $221 \text{ mg m}^{-2} \text{ d}^{-1}$ ).

Overall the  $CH_4$  degassing budget is low ( $27.09 \text{ t km}^{-2} \text{ y}^{-1}$ ) when compared with other Italian mud volcanoes. This could be related to a relative low emission activity during the period of the geochemical survey and to a more homogeneous dilution of surface distribution of the emission points.

Chemical and isotopical composition of the gas discharged from the active gryphons is methane-dominated and the thermogenic signature (ranging from -41 to -47‰) suggests a deep reservoir source. This conclusion

1 is supported by noble-gas measurements (He, Ne, Ar, Kr, Xe) conducted in the pore water phase of the  
2 emitted mud, indicating a secondary gas exchange occurring at a depth of a few kilometers.

3 The geochemical anomalies found in this study, successfully predicted the occurrence of new degassing  
4 phenomena towards the NE sector of the caldera. Indeed recently new manifestations of mud and gas  
5 emissions appeared in the north-eastern edge of the caldera.  
6  
7  
8  
9

10  
11 **Keywords:** *Mud Volcano; soil gas survey; gas geochemistry; thermogenic methane; Po Plain*  
12  
13

## 14 15 **1. Introduction**

16  
17  
18 Mud volcanoes are the surface expression of subsurface processes characterized by movements of large  
19 masses of sediments and fluids, collectively indicated as “sedimentary volcanism” (Mazzini and Etiope,  
20 2017). Dormant mud volcanoes are geological structures built by the surface emission of mud breccia  
21 (coarse- and fine-grained sedimentary particles and rock clasts), formation water and hydrocarbons expelled  
22 from pressurized deep sources through structurally controlled conduits (e.g., Kopf, 2002). Mazzini and  
23 Etiope (2017) highlighted two important mechanisms essential for the formation of mud volcanism: 1)  
24 gravitational instability, resulting from the fast burial of fluids and organic-rich sediments and 2) the  
25 overpressure produced by the generation of hydrocarbons at depth. The presence of efficient seals allows  
26 overpressured fluids to be entrapped in isolated geological compartments.  
27  
28  
29  
30  
31  
32

33 Mud volcanoes are worldwide diffused, particularly in active and passive margins, deep sedimentary basins  
34 related to active plate boundaries, as well as delta regions, or areas involving e.g. salt diapirism, as part of  
35 petroleum systems (Etiope, 2015).  
36  
37

38 In Italy, mud volcanoes occur along the external compressive margin of the Northern (Pede–Apennine  
39 margin of Emilia-Romagna) and Central Apennine (eastern Marche-Abruzzo) and in Sicily (Pellegrini et al.,  
40 1982; Capozzi et al., 1994; Martinelli, 1999; Martinelli and Judd, 2004; Etiope et al., 2007; Tassi et al.,  
41 2012). If compared to other world examples, most of the Italian mud volcanoes are small sized and seldom  
42 exhibit periodic explosions (e.g. the 2014 tragedy occurred at Macalube mud volcano in Sicily; Mazzini and  
43 Etiope, 2017, or at Santa Barbara mud volcano, Madonia et al.; 2011), which are often related to important  
44 seismic activity (Accaino et al., 2007).  
45  
46  
47  
48  
49

50 Nirano mud volcano (NMV), located inside the wider Regional Natural Reserve of Salse di Nirano, is  
51 distributed over an area of about 10 ha near the Nirano village (Fiorano Modenese). The number of vents  
52 present at NMV, as well as their shape and location, vary over the time (Martinelli and Judd, 2004), even if  
53 their age increases from SW to NE. Currently exist five main active sites, composed of a changing number of  
54 individual active gryphons, and numerous pools all defining structural alignments trending ENE-WSW and  
55 running subparallel to the Pede-Apennines thrust (Bonini, 2007, 2008). The gryphons have subcircular shape  
56 with a basal radius up to 20 m and a meter-scaled bubbling upper part that may reach up to 3 m in height.  
57  
58  
59  
60  
61  
62  
63  
64  
65

1 Water, mud and small fractions of liquid hydrocarbons are periodically emitted at the gryphons and pools  
2 scattered over an elliptical depression (~500 m long, 350 m wide, ≤60 m deep) (Sciarrà et al., 2015a and  
3 references therein). Discharged fluids contain also small marine fossils (calcareous nanoplankton), sub-  
4 millimetric fragments of claystones and carbonates. These represent the brecciated clasts of the formations  
5 intersected by the feeder conduit during the rise of overpressured fluids (Bonini, 2008).  
6

7  
8 The NMV is known since ancient records and has been described by historians (Stoppani, 1873; Coppi,  
9 1875; Pantanelli and Santi, 1896; Biasutti, 1907; Barbieri, 1947; Mucchi, 1966, 1968) and investigated for  
10 various aspects including: i) mineralogy (Ferrari and Vianello, 1985); ii) mud volcanism related to tectonic  
11 activity (Gorgoni et al., 1988; Gorgoni, 2003; Bonini 2007, 2008, 2009 and 2012; Manga and Bonini, 2012;  
12 Lupi et al., 2016); iii) geology and geomorphology (Bertacchini et al., 1999; Castaldini et al., 2003; 2005;  
13 2007; 2011); and iv) microbiology (Heller et al., 2011; 2012), contributing to create an important database on  
14 its evolution.  
15  
16  
17  
18

19 From a geochemical point of view, research surveys mainly focused on the chemical and isotopic  
20 characterization of fluids emitted by active seepage sites. Minissale et al. (2000) investigated chemical and  
21 isotopic characteristics of natural gas and thermal water of Northern Apennines, among those Nirano. They  
22 found that at NMV free gases are mainly methane (>98%) with small amounts of other hydrocarbons, carbon  
23 dioxide and nitrogen. The carbon isotope ratios ( $\delta^{13}\text{C-CH}_4 = -46\text{‰ PDB}$ ) indicate a thermogenic origin.  
24 Discharged waters from volcanoes are brackish ( $\text{TDS} = 7.12 \text{ g L}^{-1}$ ) suggesting a marine origin. Oxygen  
25 isotope ratios ( $\delta^{18}\text{O} = 5.5\text{‰ SMOW}$ ), and hydrogen isotope ratios ( $\delta\text{D} = 4.0 \text{‰ SMOW}$ ), joint to isotopic  
26 composition of strontium and tritium, indicate negligible input of meteoric waters in the system and confirm  
27 the connate origin of the water (Cipriani et al., 2017). In this study, Minissale et al. (2000) conclude that the  
28 fluids discharged are probably syngenetic with the Plio-Pleistocene “Argille Azzurre” Formation cropping  
29 out in the study area. Moreover, authors noted that the seeping gas is relatively enriched in helium, and  
30 suggested an enrichment in crustal radiogenic  $^4\text{He}$  and long underground residence times. Etiope et al. (2007)  
31 reported free gas and isotopic composition of all main terrestrial mud volcanoes and other methane seeps in  
32 Italy, among those Nirano. Their results ( $\delta^{13}\text{C-CH}_4 = -46\text{‰}$ ,  $\delta\text{D-CH}_4 = -186\text{‰}$ ) is in agreement with  
33 Minissale et al. (2000). Heller et al. (2011, 2012) carried out chemical and microbiological analysis of mud  
34 and free gas from one of the active gryphons, founding the presence of anaerobic oxidation of methane. Tassi  
35 et al. (2012) presented gas geochemical and isotopic composition of  $\text{C}_2\text{--C}_{10}$  alkane, cyclic and aromatic  
36 compounds. They found that methane is by far the most abundant component with the presence of more than  
37 20 different cyclic compounds with concentrations up to several  $\mu\text{mol mol}^{-1}$ . Cyclic compounds are likely  
38 formed by: *i*) thermal cracking and *ii*) uncompleted aromatization of alkanes occurring at depth >3 km and  
39 temperatures not exceeding 120 – 150 °C.  
40  
41  
42  
43  
44  
45  
46  
47  
48  
49  
50  
51  
52  
53  
54

55 Despite the work done, no studies have been completed to investigate the soil gas distribution in relation to  
56 possible tectonic discontinuities and characterize micro- and macro-seepage for both  $\text{CO}_2$  and  $\text{CH}_4$ . Soil–gas  
57 geochemistry represents a widely used technique to detect seeping gases and identify preferential migration  
58 pathways and active tectonic structures such as buried faults and fractured fields (e.g. Baubron et al., 2002;  
59  
60  
61  
62  
63  
64  
65

Ciotoli et al., 2005, 2016; Quattrocchi et al., 2012; Sciarra et al., 2015b, 2017, 2018; Valente et al., 2018).

The output of seepage is important in the framework of geogenic emissions of greenhouse gases since mud volcanoes represent the second natural source of CH<sub>4</sub> in the atmosphere (Etiope, 2004; Saunois et al., 2016).

It is estimated that during their dormancy mud volcanoes globally emit (i.e. from seeps, gryphons and micro-seepage) 5 to 20 Mton y<sup>-1</sup> (Mazzini and Etiope, 2017 and references therein).

The goal of our study is to fill some of the existing gaps of knowledge of the NMV presenting results of an extensive geochemical survey. More precisely this study aims to: i) define the natural degassing value (baseline or background) in the studied area, ii) identify enhanced permeability sectors possibly linked to preferential leakage pathways such as fault and/or fracture systems, iii) discriminate the migration processes and the carrier role of the various gaseous species, and, iv) quantify the CO<sub>2</sub> and CH<sub>4</sub> fluxes from soils and active cones aiming to an accurate estimation of CO<sub>2</sub> and CH<sub>4</sub> seepage output to the atmosphere.

## 2. Stratigraphic and geological setting

The NMV is located in the low hill territory of the Modena Apennine (Fig. 1), upon an anticline structure with a NW–SE axis associated to the Pede-Apennines thrust (e.g., Benedetti et al., 2003; Bonini, 2008). The Modena Apennine margin is characterized by prevalently compressive structures (Emilia Folds; Pieri and Groppi, 1981; Gasperi et al., 1989) produced by northbound translational movements (occurring mainly during the Messinian and Pliocene). In particular, the study area is characterized by the presence of two systems of tectonic discontinuities (fault and/or fractures) NW-SE and SW-NE oriented, respectively (Fig. 1).

The NMV develops on the bottom of a caldera-like structure, with a maximum diameter of about 500 meters. The caldera collapse is believed to have formed within the Plio-Pleistocene succession (Capozzi et al. 1994; Martinelli and Rabbi, 1998; Castaldini et al. 2005; Accaino et al. 2007), possibly following different paroxysmal events of fluid and mud emission. Bonini (2008) describes this caldera as the result of the collapse of the top portion of a mud diapir arising to the surface, similarly to what happens in some submarine structures (e.g. Henry et al. 1990).

Clayey and sandy marine sediments (Argille Azzurre formation, from Middle Pliocene to Lower Pleistocene) outcrop around the NMV. These deposits overlay, from the top (Fig.1): i) sandstones, claystones and conglomerates belonging to the Epi-Ligurian Units; ii) shales of Ligurian Units, and iii) sandstones and siltstones of Marnoso Arenacea formation (Miocene). The latter formation constitutes the deep reservoir (about 2 km depth) from which pressurized fluids migrate along high-angle thrust faults toward surface, accumulating at shallow depths within the Epi-Ligurian Units (Bonini, 2008).

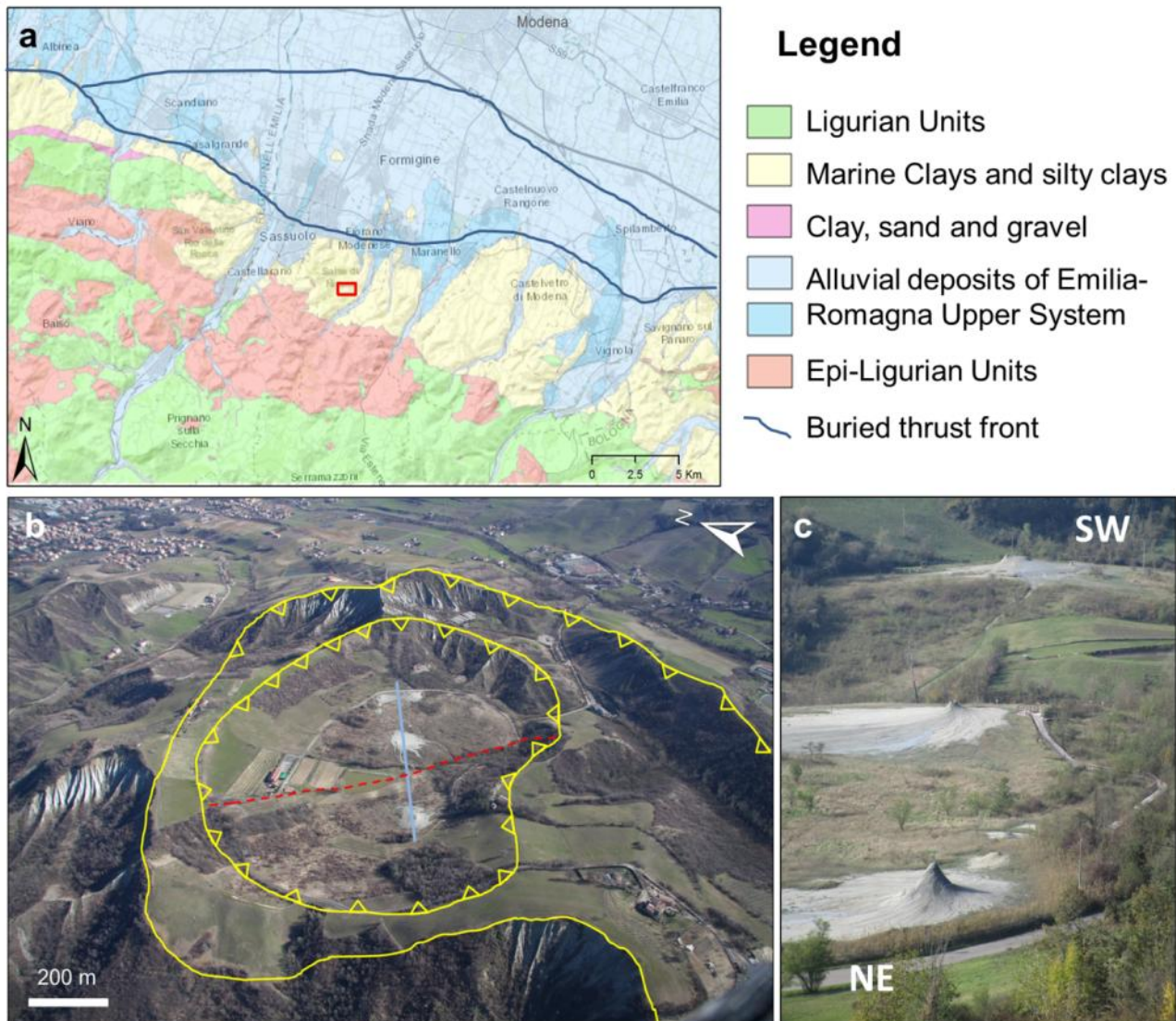


Figure 1. a) Geological map of the Pedemontane region. The Pedemontane thrust is marked by the bold blue line (<http://geoportale.regione.emilia-romagna.it/it/mappe>); b) detailed map of NMV showing caldera ring faults (yellow line), preferential alignment of main gryphons (blue line), fault inferred by morphological evidence (dashed red line); c) picture of the gryphon clusters and their preferential NE-SW alignment.

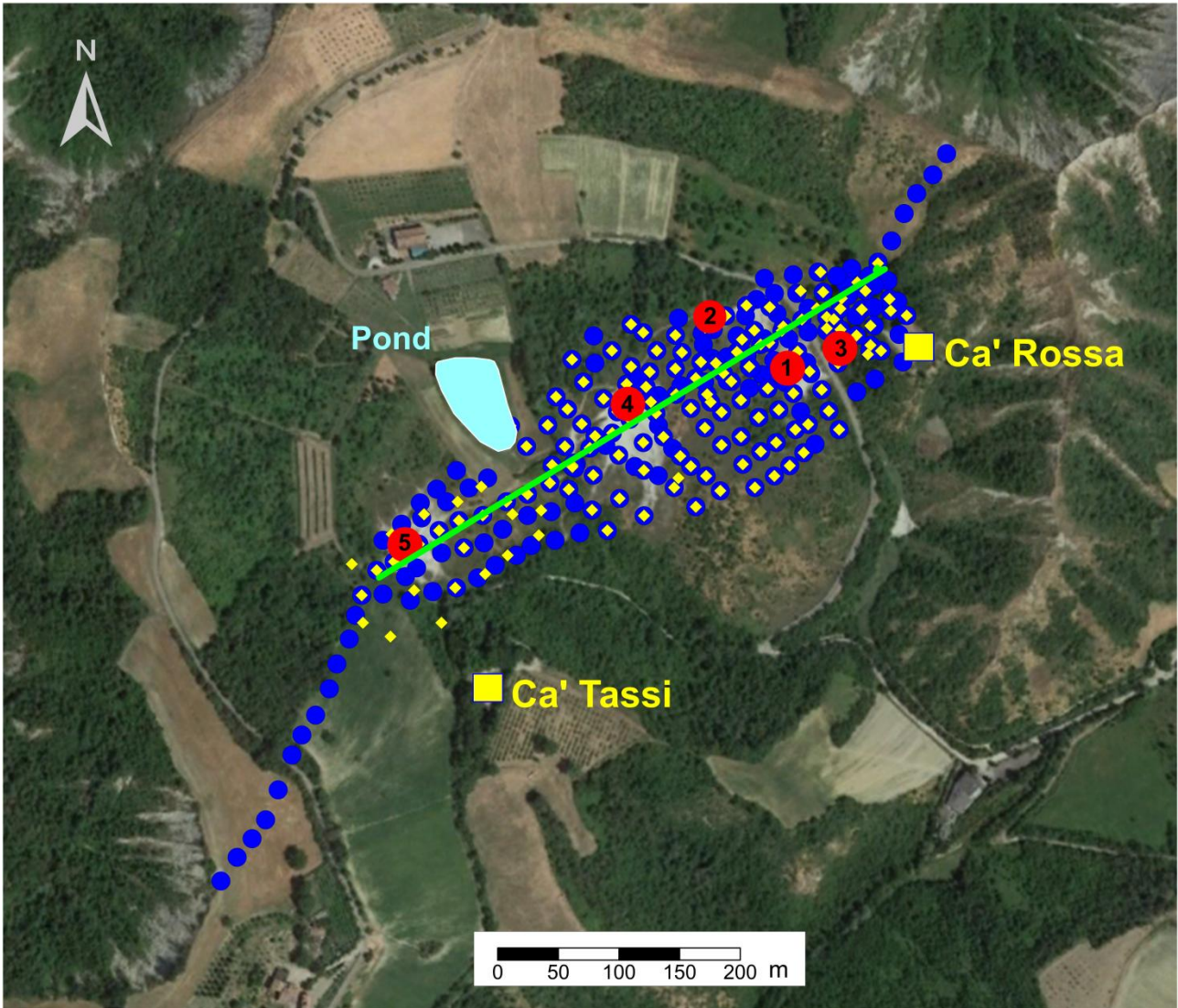
### 3. Methodology

147 soil gas concentration (He, Ne, H<sub>2</sub>, O<sub>2</sub>, N<sub>2</sub>, CH<sub>4</sub>, CO<sub>2</sub>, light hydrocarbons and <sup>222</sup>Rn) and 209 CO<sub>2</sub> and CH<sub>4</sub> flux measurements were carried out during several surveys in spring-summer 2015 inside the NMV. To determine the soil degassing background, 18 additional flux measurements were measured outside the area that limits the mud volcanic caldera. Measurements covered an area of 78742 m<sup>2</sup>, following a regular grid with steps of 20 and 40 m for fluxes and soil gas measurements, respectively (Fig. 2). Free gas samples were collected from five vents located in different sectors of NMV for chemical and isotopical analysis (Fig.2).

The free gas flux was estimated by a funnel positioned above the bubbling point and connected to a 1.5 L calibrated vial through a silicon tube. The degassing was assessed measuring the time needed by the gas to

1 replace the volume of water filling the bottle. This procedure was repeated several times, in order to obtain a  
2 reliable average of the measurements.  
3

4 Finally, in order to compare the results of the present study with the ones obtained by Lupi et al. (2016) by  
5 means of geoelectrical investigations, detailed fluxes and soil gas measurements were carried out along a  
6 SW-NE profile (20 m spacing between measurements) crossing five active emission structures (Fig. 2). This  
7 profile overlaps Profile 1 performed by Lupi et al. (2016) to investigate the subsurface structure of the NMV  
8 by 2D Electrical Resistivity Tomography (ERT).  
9  
10  
11  
12



13  
14  
15  
16  
17  
18  
19  
20  
21  
22  
23  
24  
25  
26  
27  
28  
29  
30  
31  
32  
33  
34  
35  
36  
37  
38  
39  
40  
41  
42  
43  
44  
45  
46  
47  
48  
49  
50  
51  
52  
53  
54  
55  
56  
57  
58  
59  
60  
61  
62  
63  
64  
65

Figure 2. Distribution of soil gas concentration (yellow diamonds), flux measurements (blue dots), SW-NE profile (green line) and location of free gas sampling on the five active sites (red dots). Ca' Tassi and Ca' Rossa are the museums of Salse di Nirano Natural Reserve.

### 3.1 Soil gas

1 Soil gas survey consists in collecting and analyzing gas samples from the vadose zone to measure the  
2 concentration of the gaseous species that permeate the soil pores. Sampling was accomplished in a period of  
3 stable and dry weather conditions, and in a short time to minimize any variations induced by different  
4 sampling periods. Soil gas samples were collected using a steel probe that was driven into the ground to a  
5 depth of 0.8 m, to avoid the major influence of meteorological variables (e.g., [Segovia et al., 1987](#); [Hinkle,  
6 1994](#)), and successively analyzed in the Fluid Geochemistry Laboratory at INGV Rome. Soil gas  
7 concentrations (He, Ne, H<sub>2</sub>, O<sub>2</sub>, N<sub>2</sub>, CH<sub>4</sub>, C<sub>2</sub>H<sub>2</sub>, C<sub>2</sub>H<sub>4</sub>, C<sub>2</sub>H<sub>6</sub>, CO<sub>2</sub>) were analyzed using a MicroGC Varian  
8 4900 CP, equipped with two Thermal Conductivity Detectors (TCD), responding to the difference in thermal  
9 conductivity between the carrier gas (He or Ar) and the sample components.

10 Radon (<sup>222</sup>Rn; half-life 3.8 days) was analyzed directly in the field using a RAD7 DurrIDGE alpha  
11 spectrometry instrument. The instrument is equipped with a solid-state alpha detector and it is connected  
12 with a hollow probe at depth of ~0.7 m. A single measurement has an average duration of 20 min, with  
13 partial readings every 5 minutes. Four measurements were completed at each site. A desiccant trap (Drierite)  
14 and an inlet filter protect the detector from soil moisture (>10%).

### 24 3.2 CO<sub>2</sub> and CH<sub>4</sub> fluxes

25 CO<sub>2</sub> and CH<sub>4</sub> fluxes were measured using the “accumulation chamber” method (e.g., [Chiodini et al., 1998](#))  
26 by means of a West System™ portable fluxmeter equipped with CO<sub>2</sub> and CH<sub>4</sub> detectors.

27 The CO<sub>2</sub> detector is a LICOR–LI820, very accurate in the range from 0 up to 600 mol m<sup>-2</sup> d<sup>-1</sup> (0–26400 g m<sup>-2</sup>  
28 d<sup>-1</sup>). The CH<sub>4</sub> flux meter is a TLD Tunable Laser Diode spectrometer (West System) that allows the  
29 measurement of flux in the range from 0.01 up to 750 mol m<sup>-2</sup> day<sup>-1</sup> (0.16–12000 g m<sup>-2</sup> d<sup>-1</sup>).

30 Data obtained directly in the field, were treated and calculated considering the variation of barometric  
31 pressure and temperature measured during the survey. The recorded concentrations measured over the time,  
32 with other parameters such as volume (0.003 m<sup>3</sup>) and surface (0.0314 m<sup>2</sup>) of the accumulation chamber,  
33 allow calculation of the CO<sub>2</sub> and CH<sub>4</sub> fluxes from the soil ([Hutchinson et al., 2000](#)).

### 42 3.3 Free gas

43 Free gases were sampled using a plastic funnel up-side-down positioned above the bubbling mud pools and  
44 connected through silicone/tygon tubes to pre-evacuated 250 mL glass flasks. Subsequently gases were  
45 analyzed using a MicroGC Varian 4009 CP. Isotopic analysis on free gas (δ<sup>13</sup>C–CO<sub>2</sub>, δ<sup>13</sup>C–CH<sub>4</sub>, δD–CH<sub>4</sub>,  
46 <sup>3</sup>He/<sup>4</sup>He, <sup>40</sup>Ar/<sup>36</sup>Ar) were performed by spectrometry at the laboratory of Istituto Nazionale di Geofisica e  
47 Vulcanologia, Sezione di Palermo. The δ<sup>13</sup>C in CO<sub>2</sub> values (expressed as δ<sup>13</sup>C–CO<sub>2</sub> ‰ vs. VPDB) were  
48 analyzed by mass spectrometry (Finningan Delta S). The analytical uncertainty and the reproducibility are  
49 ±0.05‰.

50 The δ<sup>13</sup>C–CH<sub>4</sub> and δD–CH<sub>4</sub> values (expressed as δ<sup>13</sup>C–CH<sub>4</sub> ‰ vs. VPDB and δD–CH<sub>4</sub> ‰ vs. VSMOW,  
51 respectively) were analyzed by mass spectrometry (Varian MAT 250) according to the procedure reported by  
52 [Schoell \(1980\)](#). The analytical uncertainty is ±0.15‰.

1 The  $^3\text{He}/^4\text{He}$  ratios (expressed as R/Ra, where R is the  $^3\text{He}/^4\text{He}$  measured ratio and Ra is the  $^3\text{He}/^4\text{He}$  ratio in  
2 the air:  $1.39 \times 10^{-6}$ ; Mamyryn and Tolstikhin, 1984), as well as  $^{40}\text{Ar}/^{36}\text{Ar}$  ratios, were determined by using a  
3 double collector mass spectrometer (VG 5400-TFT) according to the method described by Inguaggiato and  
4 Rizzo (2004). The analytical error is  $\pm 1\%$ .  
5  
6  
7

### 8 3.4 Noble-gas analysis on mud 9

10 Mud samples for a comprehensive noble-gas analysis (i.e., He, Ne, Ar, Kr, Xe as well as the  $^3\text{He}/^4\text{He}$ ,  
11  $^{20}\text{Ne}/^{22}\text{Ne}$ , and  $^{36}\text{Ar}/^{40}\text{Ar}$  isotope ratios) in the water phase were collected in copper tubes sealed airtight by  
12 two metal clamps (Brennwald et al., 2003; 2013; Tomonaga et al., 2011; 2013; 2014; 2015; Tyroller et al.,  
13 2016). Sample preparation in the laboratory was carried out according to the method of Tomonaga et al.  
14 (2011). The copper tube containing each sample was divided into two aliquots by placing four additional  
15 metal clamps. Each aliquot was then centrifuged to separate the water from the sediment. After the  
16 centrifuging process, one aliquot was pinched off at a position located slightly above the sediment-water  
17 interface, which was determined by visual inspection by opening the copper tube of the other aliquot  
18 (Tomonaga et al., 2011). Noble-gas analysis was conducted only on the separated water according to the  
19 well-established experimental protocols commonly used to determine noble-gas abundances in water  
20 samples at the Noble Gas Laboratory of ETH Zurich (Beyerle et al., 2000).  
21  
22  
23  
24  
25  
26  
27  
28  
29

### 30 3.5 Data treatment 31

32 Preliminary analysis involved the calculation of standard statistical parameters to evaluate the basic  
33 characteristics of the data, define a background value and its anomaly threshold. Therefore, to identify  
34 statistical populations for each parameter, all collected data were processed with a statistical approach, by  
35 means of normal probability plot (NPP). According to Sinclair (1974, 1991), the NPP provides a good  
36 method to distinguish different populations and a more objective approach to statistical anomaly threshold  
37 estimation (Ciotoli et al., 2007).  
38  
39  
40

41 On the basis of NPP classification contour maps of investigated gas species were elaborated by kriging  
42 interpolation method (e.g., Bergfeld et al., 2001), derived from empirical semivariograms.  
43

44 The acquired flux measurements were used to estimate the total output (Q) of the  $\text{CO}_2$  and  $\text{CH}_4$  directly  
45 discharged by soil according to Chiodini and Frondini (2001) approach (Eq.1). The emission rates (expressed  
46 in t/day) were calculated by summing the contribution of each population, computed by multiplying the  
47 mean flux value for the area covered by each population (Eq.1). The budget calculation does not consider the  
48 amount due to the soil respiration component (background) and vent emissions (macroseeps).  
49  
50  
51  
52

$$53 \quad Q_{\text{CO}_2, \text{CH}_4} = \sum \Phi_{\text{CO}_2, i} \Phi_{\text{CH}_4, j} \times A_{i, j} \quad \text{Eq.1}$$

54 where  $\Phi_{\text{CO}_2, i}$  represents the average  $\varphi_{\text{CO}_2}$  of the i-th population,  $\Phi_{\text{CH}_4, j}$  represents the average  $\varphi_{\text{CH}_4}$  of the j-  
55 th population, and  $A_{i, j}$  is the calculated area covered by each population.  
56  
57  
58  
59  
60  
61  
62  
63  
64  
65



#### 4. Results and discussion

The main statistics of sampled data are reported in Table 1. N<sub>2</sub> and O<sub>2</sub> were not reported in Table 1 and discussed as their average values match essentially the atmospheric composition (i.e., 20.95 vol.% and 78.08 vol.%, respectively; [Hermansson et al., 1991](#); [Etiopie and Lombardi, 1995](#)).

**Table 1.** Descriptive statistics of CO<sub>2</sub> and CH<sub>4</sub> fluxes, and soil gas concentration of He, Ne, H<sub>2</sub>, CH<sub>4</sub>, CO<sub>2</sub> and <sup>222</sup>Rn measured in the NMV area.

	$\phi\text{CO}_2$ (g m <sup>-2</sup> d <sup>-1</sup> )	$\phi\text{CH}_4$ (mg m <sup>-2</sup> d <sup>-1</sup> )	He (ppmv/v/v)	Ne (ppmv/v/v)	H <sub>2</sub> (ppmv/v/v)	CH <sub>4</sub> (ppmv/v/v)	CO <sub>2</sub> (vol.%)	<sup>222</sup> Rn (Bq m <sup>-3</sup> )
N	227	227	147	147	147	147	147	147
Mean	17.9	220.9	5.83	13.3	2.7	290.9	0.92	3362
Median	16.68	0.01	5.5	13.8	1.4	21.4	0.78	838
Minimum	0.00	-7.27	2.8	2.85	0.08	0.44	0.04	0.00
Maximum	91.41	3208.5	17.9	26.9	38.8	6212.1	5.5	28800
LQ	9.33	0.003	5.2	12.4	0.9	4.6	0.3	202
UQ	22.7	0.028	6.3	15.3	2.7	355.8	1.1	2625
Variance	165	6489667	1	19	20	389744	1	37519204
Std. dev.	12.9	2547.5	0.9	4.3	4.5	624.3	0.86	6125.3
Skewness	2.15	13.55	4.84	-0.16	5.48	3.86	2.58	2.66

Statistical parameter of  $\phi\text{CH}_4$ , CH<sub>4</sub>, <sup>222</sup>Rn and  $\phi\text{CO}_2$  (Table 1) have a dispersed distribution as highlighted by the high values of standard deviation (2547.5, 624.3, 6125.3 and 12.9, respectively). On the other hand,  $\phi\text{CO}_2$ , <sup>222</sup>Rn and CH<sub>4</sub> show high skewness values (2.15, 2.66 e 3.86, respectively), suggesting the presence of outliers. The  $\phi\text{CH}_4$  and, to a lesser extent, He and H<sub>2</sub> have a skewness value (13.55, 4.84 and 5.48, respectively) showing a clear dispersed distribution with anomalous values.

#### 4.1 Soil gas concentrations

The distribution of soil gas, in particular trace gases as <sup>222</sup>Rn, He e H<sub>2</sub>, was investigated to identify potential faults and/or fractures related to preferential migration pathways and the possible interaction between deep reservoirs and surface.

1 Normal probability plots were used to identify background, anomalous and outliers values. In particular  
2 values above 2 vol.% for CO<sub>2</sub>, 10 ppmv/v for H<sub>2</sub>, 40 ppmv/v for CH<sub>4</sub>, 2500 Bq m<sup>-3</sup> for Rn, 5.5 ppmv/v for  
3 He and 18 ppmv/v for Ne have been considered as anomalous.  
4

5 The main statistical parameters of Rn, CO<sub>2</sub>, CH<sub>4</sub> and He data collected in the NMV were compared to those  
6 measured in the cultivated areas of Modena Province (Sciarra et al., 2013) and obtained by the same  
7 methodology, in order to have a homogeneous database as a reference.  
8

9 Concentrations of radon and carbon dioxide show mean and median that are lower compared to reference  
10 values. In particular, mean <sup>222</sup>Rn values for NMV are 3362 Bq m<sup>-3</sup> versus 4800 Bq m<sup>-3</sup>, while CO<sub>2</sub>  
11 concentration has a mean of 0.92 vol.% with respect to 2.31 vol.% of reference values.  
12

13 On the contrary, methane concentrations are about two orders of magnitude higher than reference values,  
14 with mean of 290 ppmv/v and median of 21.4 ppmv/v versus 6.01 and 0.15 ppmv/v, respectively, and H<sub>2</sub> is  
15 about one order of magnitude higher (2.7 and 1.4 ppmv/v) than those reported by Sciarra et al. (2013; 0.44  
16 and 0.31 ppmv/v). The He mean concentration (5.83 ppmv/v) substantially agrees with both atmospheric and  
17 reference values.  
18

19 Spatial distribution of CO<sub>2</sub> (Fig. 3a) shows anomalous values (> 2 vol.%) in the NE sector of the study area,  
20 where the mud volcano activity is more recent (west to Ca' Rossa museum). Other weak high values are  
21 found in the central part of the crater zone close to a large water pond.  
22

23 Contour map of <sup>222</sup>Rn (Fig. 3b) highlights two zones in the NMV characterized by high values (> 14000 Bq  
24 m<sup>-3</sup>). The first one is located in the NE area, in correspondence of a CO<sub>2</sub> anomaly while the second is located  
25 in the SW of the survey area, between the south-westernmost gryphon site (point 5) and the water pond.  
26

27 CH<sub>4</sub> and He (Figs. 3c and e) show a similar spatial distribution, with high values (>2500 ppmv/v and 6  
28 ppmv/v, respectively) in the northern part of the study area (points 2 and 4) and close to Ca' Rossa (point 3).  
29 This observation suggests that both gas species may be sourced from the same layer, with methane acting as  
30 carrier.  
31

32 H<sub>2</sub> anomalous values (> 16 ppmv/v) are distributed in three distinct areas located in the NE, N and SW areas  
33 in agreement with higher values of the other gas species (Fig. 3d).  
34

35 The Ne distribution (Fig. 3f) shows a preferential alignment of anomalous values along the oblique line  
36 crossing the study area from SW to NE. This gas species is indicative of circulation path of shallower fluids  
37 probably linked to a surficial fracturation system.  
38

39 Spatial distribution of the highest values for CO<sub>2</sub>, <sup>222</sup>Rn, CH<sub>4</sub>, He, Ne e H<sub>2</sub> highlights a general association  
40 among the considered species in the NE sector of the studied area, whereas <sup>222</sup>Rn, Ne, H<sub>2</sub> show a good  
41 correlation also in the SW sector.  
42

43 These two regions are located at the extremities of the NE-SW aligned seepage sites and coincide with the  
44 morphological edges of the caldera. We suggest that these preferential locations may result from: 1) a sealing  
45 effect by the mud mostly extruded in the central part, and/or 2) by a tectonic control operated by the caldera  
46

collapse faults that facilitate the preferential rise of deep fluids. A similar mechanism has been already suggested for other mud volcano sites (Mazzini et al., 2009; Mazzini and Etiope, 2017).

Since  $^{222}\text{Rn}$  and other trace gases (He and  $\text{H}_2$ ) are considered suitable fault tracers and  $\text{CO}_2$  and  $\text{CH}_4$  are believed to act as carriers for these gases (Beaubien et al., 2003; Sciarra et al., 2015b; 2017; 2018; Ciotoli et al., 2016), their association suggests the presence of two areas characterized by high permeability zones from which gas upraise at surface.

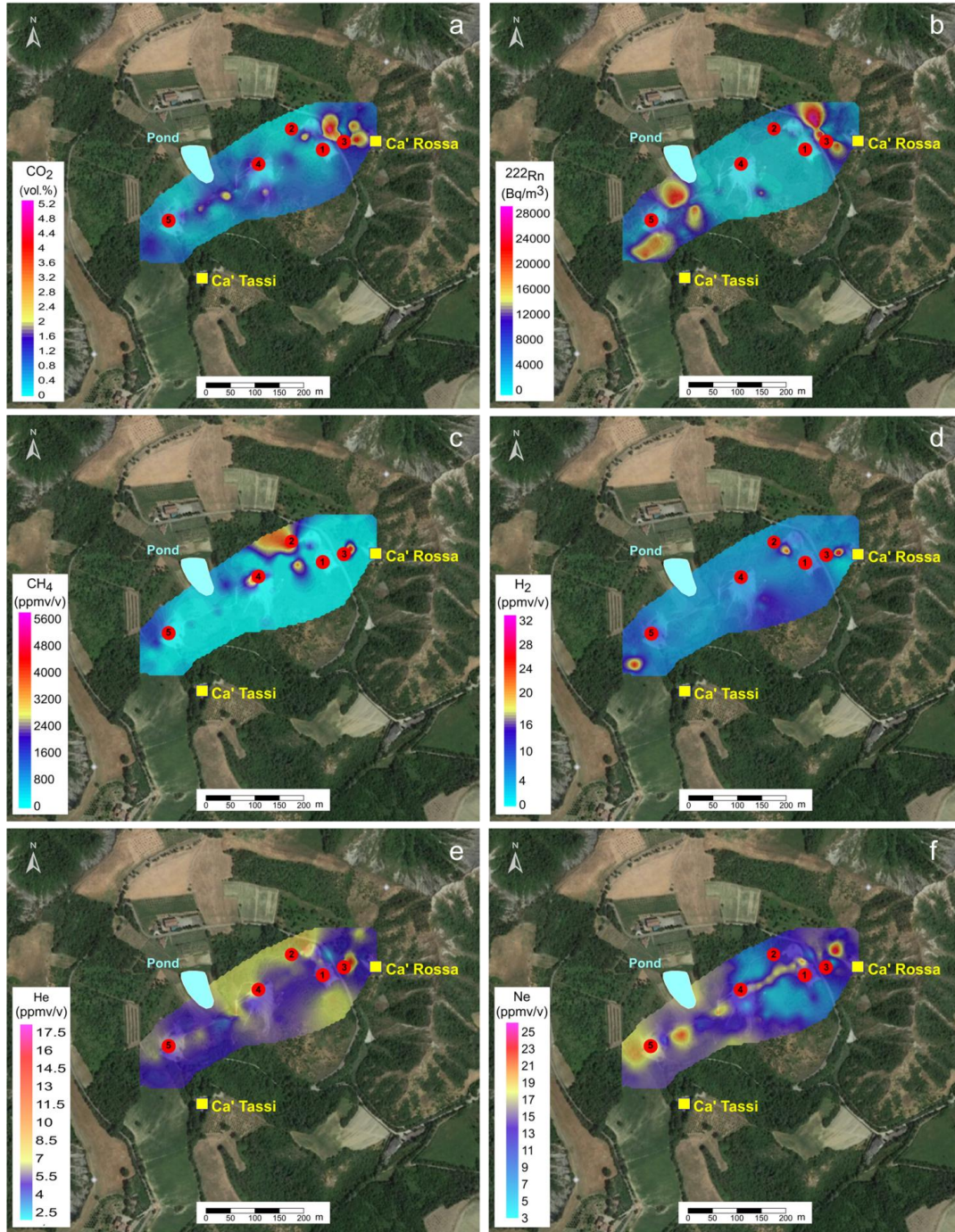


Figure 3 – Contour maps for the concentrations of investigated gas species: a)  $\text{CO}_2$ ; b)  $^{222}\text{Rn}$ ; c)  $\text{CH}_4$ ; d)  $\text{H}_2$ ; e) He; f) Ne, show the presence of high soil gas values at the edges of the caldera, a good spatial correlation between trace gas elements and their carrier gases, and along the NE-SW aligned gryphons distribution.

## 4.2 CO<sub>2</sub> and CH<sub>4</sub> flux measurements

Statistical elaboration on the basis of NPP allowed to define threshold anomaly for  $\phi\text{CO}_2$  ( $20 \text{ g m}^{-2} \text{ d}^{-1}$ ), and  $\phi\text{CH}_4$  ( $44 \text{ mg m}^{-2} \text{ d}^{-1}$ ).

The average CO<sub>2</sub> exhalation flux (Table 1) reveals values lower than those measured in cultivated areas of the Modena Province ( $17.9$  vs.  $21.9 \text{ g m}^{-2} \text{ d}^{-1}$ ; [Sciarra et al., 2013](#)). The highest values are located in the NE sector of the studied area, where the mud volcano activity is more recent (around Ca' Rossa) and in the central part of the area, in correspondence of the water pond and the morphological slope. A focused anomaly is located in the SW edge of the NMV (Fig. 4a). Flux measurements performed outside the area hosting the mud volcano (blue dots in Fig. 4a) range from 4 to  $20.22 \text{ g m}^{-2} \text{ d}^{-1}$ , within the background values of those measured inside the crater zone.

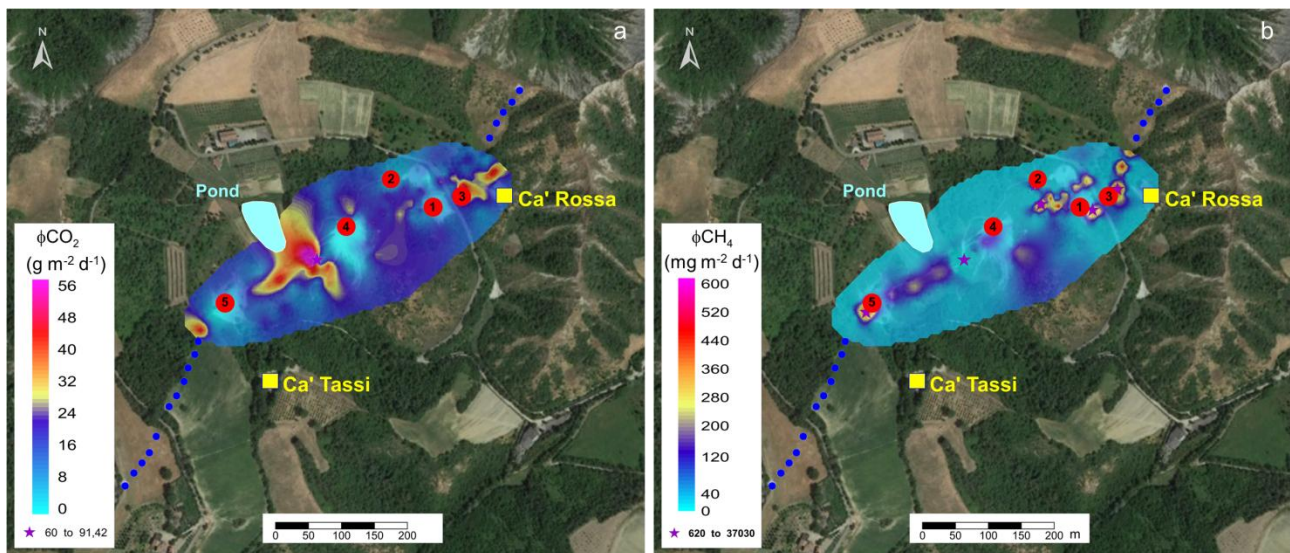


Figure 4– Distribution of flux measurements for a)  $\phi\text{CO}_2$  and b)  $\phi\text{CH}_4$  highlight the presence of more intense degassing in coincide with the morphological edges and the slope of the caldera.

Methane micro-seepage shows average values significantly lower than those measured in cultivated areas of the Modena Province ( $220$  vs.  $670 \text{ mg m}^{-2} \text{ d}^{-1}$ ; [Sciarra et al., 2013](#)). The highest values (from  $400$  to  $3200 \text{ mg m}^{-2} \text{ d}^{-1}$ ) are distributed along the oblique axis crossing the area with a NE-SW trend. Flux measurements performed outside the NMV (blue dots in Fig. 4b) are characterized by background values ranging from  $2.38$  to  $42.61 \text{ mg m}^{-2} \text{ d}^{-1}$ .

The total gas emission rates over the surveyed surface ( $A_{tot} = 0.0787 \text{ km}^2$ ) have been computed following the [Chiodini and Frondini \(2001\)](#) approach (Eq.1). Results give  $299.3 \text{ t/yr}$  for CO<sub>2</sub> ( $Q_{\text{CO}_2}$ ) and  $2.13 \text{ t yr}^{-1}$  for CH<sub>4</sub> ( $Q_{\text{CH}_4}$ ).

The free gas flux, measured for the most recent active seeps at point 3 (Fig. 5), revealed an emission rate of 64.8 L h<sup>-1</sup> (or 1.8 x 10<sup>-5</sup> m<sup>3</sup> s<sup>-1</sup>) constituted by 97% of CH<sub>4</sub> and 1% of CO<sub>2</sub> (see Section 4.4). The daily emissions from the gryphon to the atmosphere are 3.299×10<sup>-5</sup> t/day for CO<sub>2</sub> and 1.08×10<sup>-3</sup> t/day for CH<sub>4</sub>. By considering emissions from other 11 historically stable active gryphons and pools that visually have a qualitatively similar degassing mode, we obtained a macroseep output of 0.14 t y<sup>-1</sup> for CO<sub>2</sub> and 4.72 t y<sup>-1</sup> for CH<sub>4</sub>.

Etioppe et al. (2007) estimated the CH<sub>4</sub> output of Nirano from macroseeps (gryphons, bubbling pools and dry seeps) and microseepage (soil diffuse degassing). Their measured macroseepage is slightly higher than the one obtained in this study (6 t y<sup>-1</sup> vs 4.72 t y<sup>-1</sup>), whereas the microseepage output is about one order of magnitude higher (i.e. 26.4 t y<sup>-1</sup> vs 2.13 t y<sup>-1</sup>). This difference may be due to the distinct investigation periods or due to the different sampling density (6 measurements within 10000 m<sup>2</sup> vs. 210 measurements within 78742 m<sup>2</sup> of this study – a difference of almost one order of magnitude). Indeed, the fluid emissions and mud activities change over the time.

With respect to other Italian mud volcanoes, the Nirano CH<sub>4</sub> macro and microseepage estimated in this study are lower than those estimated for Regnano (5 t y<sup>-1</sup> and 29 t y<sup>-1</sup>, respectively; Table 2), located about 20 km far to Nirano and about one order of magnitude lower than Macalube (Sicily; Table 2).

**Table 2.** Output of  $\phi$ CH<sub>4</sub> from macroseeps and microseeps.

Site	Area (m <sup>2</sup> )	N. Vents	Macroseep output (t/yr)	Microseepage output (t/yr)	N. meas. microseepage	Output (t/yr)
Regnano*	5800	8	5	29	11	34
Nirano*	10000	18	6	26.4	6	32.4
Macalube*	1400000	69	20	374	9	394
Nirano (this study)	78742	12	4.72	2.13	210	6.85

\*: from Etioppe et al. (2007)



Figure 5 – Active seepage sites at the NMV. a-b) landscape, c-d) particular of bubbling phenomenon from sampling points 4 and 2, respectively, e) mud pool of point 3, f) point 1, g-h) point 5.

### 4.3 SW-NE oblique profile

Detailed fluxes and soil gas measurements (20 m spaced) were carried out along a 550 m long profile intersecting five active mud emission areas. The SW-NE oriented profile (Fig. 2) follows Profile 1 performed by Lupi et al. (2016) using 2D Electrical Resistivity Tomography (ERT).

In order to highlight the trend of different gas species and find similarities in their spatial distribution, soil gas concentrations and flux profiles were compared with the ERT data (Fig. 6).

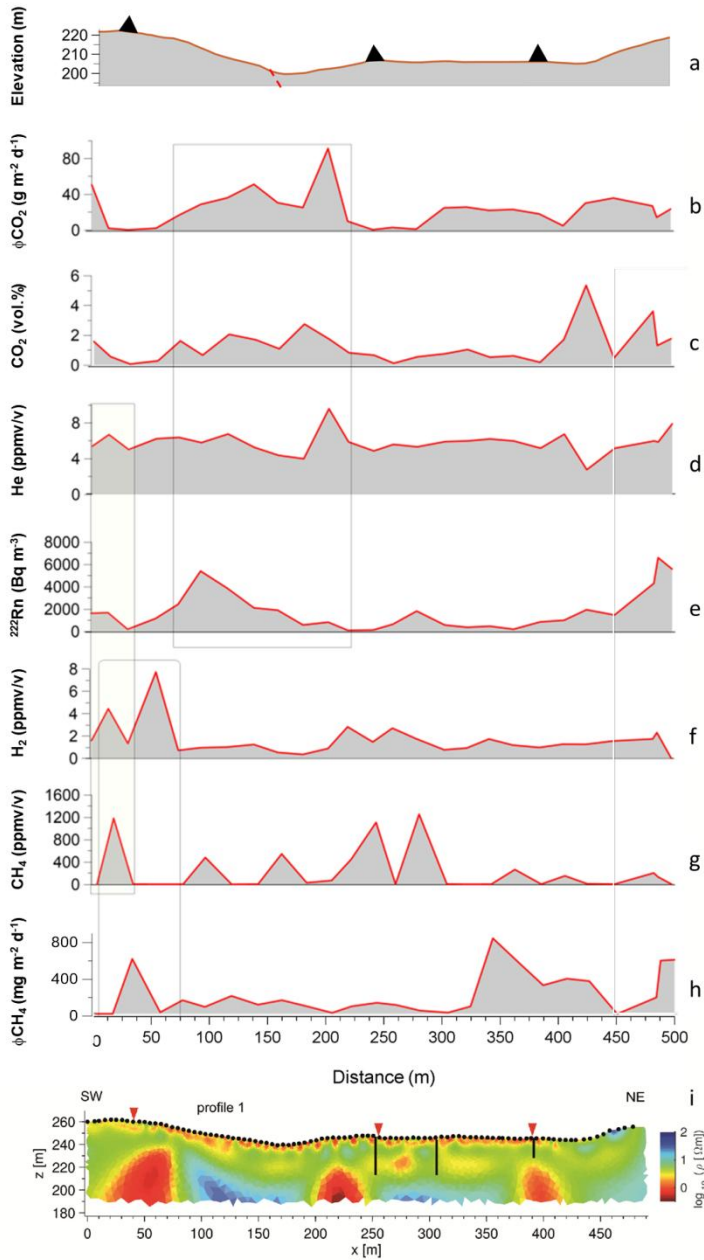
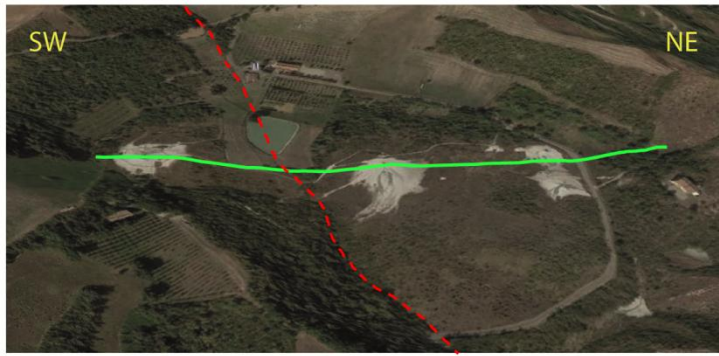


Figure 6 –Google Earth image of the oblique SW-NE profile (green line), the inferred fault (red dashed line) described in figure 1, with the completed measurements of: a) vertically exaggerated topography profile, b)  $\phi\text{CO}_2$ , c)  $\text{CO}_2$ , d) He, e)  $^{222}\text{Rn}$ , f)  $\text{H}_2$ , g)  $\text{CH}_4$ , h)  $\phi\text{CH}_4$ , i) ERT profile 1 (Lupi et al., 2016).

$\phi\text{CO}_2$ ,  $\text{CO}_2$ , He and  $^{222}\text{Rn}$  show high values in the sectors between 80- 230 m. This interval is characterized by a prominent 15 m high escarpment with NW-SE orientation, likely related to subsidence dynamics ongoing in the central area. The presence of these tectonic structures is likely facilitating the gas uprising.

Anomalous values of  $\text{CO}_2$ , He,  $^{222}\text{Rn}$ ,  $\text{H}_2$  and  $\phi\text{CH}_4$  are also concentrated between 400 m (gryphon 1) and the end of the profile where new mud emissions appeared in October 2015.

In contrast,  $\text{H}_2$ ,  $\text{CH}_4$  and  $\phi\text{CH}_4$  show high values between 0 – 70 m, and around 10-20m is present a good correlation among He,  $^{222}\text{Rn}$ ,  $\text{H}_2$  and  $\text{CH}_4$  (i.e. in the area around gryphon 5).

The highest soil gas concentrations positively correlate with the three dome-shaped conductive anomalies mapped by Lupi et al. (2016) at ~20m depth.

Depending on the combination of gas species anomalies, it is possible to distinguish if these are related to local conditions (e.g. lithology, permeability), or to gas uprising along preferential pathways. Soil gas distributions suggests the presence of sectors characterized by high permeability where  $\text{CO}_2$  and  $\text{CH}_4$  play a dominant role as carrier gases for advective transport and redistribution of trace gases (e.g., He,  $^{222}\text{Rn}$ ,  $\text{H}_2$ ). Indeed, Martinelli and Judd (2004) suggest that the decay rate of  $^{226}\text{Ra}$  to  $^{222}\text{Rn}$  does not vary with time, so changes in the  $^{222}\text{Rn}$  emission rate must result from variations in the expulsion velocity of the fluids. The fluids are confined within the source rocks, consequently changes in the pore pressure caused by crustal movements explain the variations in fluid expulsion velocity (Martinelli and Judd, 2004).

#### 4.4 Free gases emitted from the gryphons

Five active gryphons were sampled for free gas chemical and isotopic analysis (Figure 2) and the analytical results are presented in Table 3.

**Table 3.** Chemical and isotopic analysis of free gas collected from 5 active gryphons in May 2015 and March 2016<sup>(\*)</sup>, and from Puianello mud volcano (gryphon 6).

Gryphon	He (ppmv/v)	Ne (ppmv/v)	$\text{H}_2$ (ppmv/v)	$\text{CH}_4$ (vol.%)	$\text{CO}_2$ (vol.%)	$\text{C}_2\text{H}_6$ (ppmv/v)	$\delta^{13}\text{C}$ - $\text{CO}_2$	$\delta^{13}\text{C}$ - $\text{CH}_4$	$\delta\text{D}$ - $\text{CH}_4$	Rc/Ra	He/Ne	$^{40/36}\text{Ar}$
1	12.7	10.5	4.1	97.92	2.1	660	13.5	-47.5	-182			
1B	21.3	0.19	3.19	99.23	0.72	456	21.1	-41.4	-182	0.021	100.52	323.3
2	7.31	11.25	1.5	99.43	0.51	129						
3*	20.4	2.85	1.92	98.94	1.1	636	21.86	-47.22	-177.3	0.02	57.2	307.1
4	7.78	11.62	1.46	91.34	8.64	89						
5	23.2	12.3	8	99.36	0.76	95						
5B*	34.82	13.82	6.06	98.97	1.01	274	21.4	-46.7	-184			
6	30.1	0.26	1.48	95.38	3.28	3350	31.3	-46.2	-184	0.03	115.68	306.3



The seeping gas is methane-dominated, typically with concentrations higher than 90%, CO<sub>2</sub> content ranging from 0.5 and 8 vol.% and light hydrocarbons (C<sub>2</sub>H<sub>6</sub>) ranging from 90 and 3350 ppm.

The isotopic composition of the sampled gas shows an argon isotopic ratios of 307-323 being slightly higher compared to the atmospheric air value (<sup>40</sup>Ar/<sup>36</sup>Ar = 298.56; Lee et al., 2006) indicating an enrichment in radiogenic <sup>40</sup>Ar (also observed in the mud pore water; see Section 4.5, Table 4). The <sup>3</sup>He/<sup>4</sup>He ratio of about 0.02 Ra suggests a crustal origin (Mamyrin and Tolstikhin, 1984) as well as the He/Ne ratio (ranging from 57 and 116; Bertrami et al, 1984). Isotopic values of methane for sites 1,3,5 (Fig. 2) show δ<sup>13</sup>C<sub>CH<sub>4</sub></sub> and δD<sub>CH<sub>4</sub></sub> values ranging from -47.5 to - 41.4‰V-PDB, and from -184 to -177‰V-SMOW, respectively. These values suggest a thermogenic origin of CH<sub>4</sub> as graphically reported in Figure 7. In the traditional δ<sup>13</sup>C<sub>CH<sub>4</sub></sub> vs. δD<sub>CH<sub>4</sub></sub> diagram (Schoell, 1980), Nirano data were compared to soil gas sampled before and after the 2012 Emilia seismic sequence (Sciarra et al., 2017) and other mud volcanoes in the Emilia Romagna Region. The comparison highlights the different origin of Nirano gas with respect to the other gas on the Modena province. Indeed, the thermogenic origin of CH<sub>4</sub> is ascribed to the decomposition of organic matter in sediments buried at more than 3000 m depth where the temperatures are higher than 100°C (e.g., Whiticar and Suess, 1990; Tassi et al., 2012). The results of this study are therefore in good agreement with those reported in the literature for most part of Italian mud volcanoes (Minissale et al, 2000; Capozzi & Picotti, 2002; Grassa et al, 2004; Etiope et al, 2007; Tassi et al., 2012).

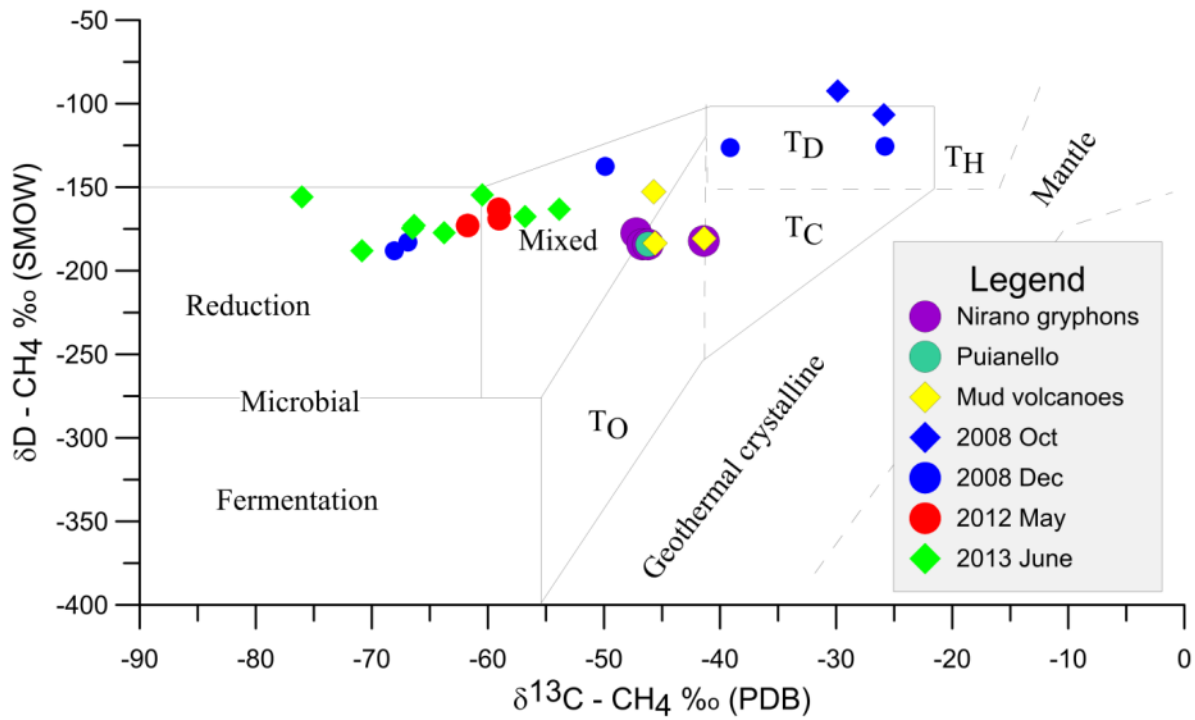


Figure 7 – Schoell diagram (Schoell, 1980) of δ<sup>13</sup>C<sub>CH<sub>4</sub></sub> vs. δD<sub>CH<sub>4</sub></sub> for free gas sampled in active gryphons of

NMV (purple dots). Blue diamonds and dots: soil gas sampled in Modena Province in 2008; red dots and green diamonds: soil gas collected during and after the 2012 Emilia seismic sequence (Sciarrà et al., 2017). Yellow diamonds: free gas sampled in other mud volcanoes in the Emilia Romagna Region (Etioppe et al., 2007).

The isotopic values of  $\delta^{13}\text{C}_{\text{CO}_2}$  ( $\approx 21\text{‰V-PDB}$ ) suggest an origin due to anaerobic oxidation of heavy hydrocarbons (Pallasser, 2000), often followed by secondary methanogenesis. This is especially true for gas samples characterized by  $\delta^{13}\text{C}_{\text{CO}_2}$  values higher than 10 ‰ V-PDB (Tassi et al., 2012). Depending on microbial communities and physico-chemical conditions of the reservoir (Wang et al., 2005), methanogenesis process are able to strongly enrich the residual  $\text{CO}_2$  in  $^{13}\text{C}$  (Etioppe et al., 2009).

#### 4.5 Noble gases in the pore water of the extruded mud

Noble gas analyses conducted in the pore water of two sampled vent sites are reported in Table 4.

**Table 4.** Noble-gas concentrations and isotope ratios measured in the water phase of the mud collected at gryphons 5 and 3. The concentrations are given in  $\text{cm}^3\text{STP}$  (STP: standard temperature and pressure of  $0^\circ\text{C}$  and 1 bar, respectively) per gram of water.

Samples	He [ $10^{-7}$ ] $\text{cm}^3\text{STP/g}$	Ne [ $10^{-7}$ ] $\text{cm}^3\text{STP/g}$	Ar [ $10^{-4}$ ] $\text{cm}^3\text{STP/g}$	Kr [ $10^{-8}$ ] $\text{cm}^3\text{STP/g}$	Xe [ $10^{-8}$ ] $\text{cm}^3\text{STP/g}$	$^3\text{He}/^4\text{He}$ [ $10^{-6}$ ]	$^{20}\text{Ne}/^{22}\text{Ne}$ [-]	$^{36}\text{Ar}/^{40}\text{Ar}$ [ $10^{-3}$ ]
NIR16-03 (Gryphon 5)	$49.9 \pm 0.3$	$155 \pm 2$	$83 \pm 4$	$95 \pm 1$	$7.00 \pm 0.07$	$1.26 \pm 0.02$	$9.80 \pm 0.01$	$3.1 \pm 0.1$
NIR16-04 (Gryphon 3)	$1.75 \pm 0.01$	$0.37 \pm 0.01$	$0.57 \pm 0.01$	$1.24 \pm 0.02$	$0.19 \pm 0.01$	$0.15 \pm 0.01$	$9.3 \pm 0.1$	$3.46 \pm 0.05$

Sample NIR16-03 appeared to be contaminated by air, as all measured concentrations are much higher than the concentrations expected for air-saturated water (ASW) for the temperature of the mud during the sampling ( $11.0^\circ\text{C}$ ). The amount of air entrapped in this sample can be estimated by least-squares fitting methods as those used to determine the so-called “noble gas temperatures” (NGT) from the measured noble gas concentrations (Aeschbach-Hertig et al., 1999; Ballentine and Hall, 1999). Such numerical methods provide a correction for the so-called “excess air” component, an excess of dissolved gases produced by the entrapment and dissolution of air bubbles often found in groundwaters. From a conceptual point of view, excess air formation does not differ from air contamination, as far as bubble dissolution is assumed to be complete (i.e., unfractionated air model). For sample NIR16-03 we could infer a total air contamination of approximately  $0.8 \text{ cm}^3\text{STP/g}$ . We used this estimation to determine the original  $^3\text{He}/^4\text{He}$  ratio in the pore water of  $3.9 \cdot 10^{-7}$  (i.e., 0.28 Ra) which is close to the value determined for sample NIR16-04 of  $1.5 \cdot 10^{-7}$  (i.e.,

0.11 Ra). These similar He isotope ratios indicate that a large share of He is radiogenic and originates from the decay of U and Th in the Earth's crust. This interpretation is in agreement with the measurement performed in the free gas phase (see Section 4.4) showing  $^3\text{He}/^4\text{He}$  ratios significantly lower than the air value (i.e., about 0.02 Ra).

Sample NIR16-04 shows atmospheric noble gas concentrations being lower than the expected ASW values calculated for the mud temperature recorded during the sampling campaign (12.8°C). Degassing (or re-equilibration) during sampling is not likely, as the sample has been acquired in March when the average air temperature was even lower than the mud temperature. The NGT calculated for this sample using the closed-system equilibration model (e.g., [Aeschbach-Hertig and Solomon, 2013](#)) assuming a salinity of 8 g/kg is about 96°C. The unconstrained NGT fitting for sample NIR16-03 delivers a (surprisingly) similar temperature of 117°C. Although statistically not robust (i.e., possibly because of fractionation processes occurring during transport of the mud to the surface), the inferred NGTs for both samples indicate that secondary gas exchange occurred with a free gas phase at depth. In light of the gas composition discussed in Section 4.4, it is reasonable to assume that this free gas phase is mainly composed by thermogenic methane produced at depths of a few kilometers. The preservation of the signature produced by secondary gas exchange at high temperatures suggests that the interaction of the mud with shallower fluids is of minor importance.

## Conclusions

A geochemical survey including 227  $\text{CO}_2$  and  $\text{CH}_4$  flux sites and 147  $\text{CO}_2$ ,  $\text{CH}_4$ , Rn, He,  $\text{H}_2$  and light hydrocarbons concentration measurements has been carried out inside the NMV in order to investigate the gas seepage from soil and estimate the  $\text{CO}_2$  and  $\text{CH}_4$  output. Moreover, free gas for chemical and isotopic analysis was collected from five active sites located in different sectors of the volcano.

Main active gryphons and seeps are distributed along a 500 m long SW-NE oriented alignment that is likely controlled by a tectonic structure providing pathway for the rise of deep fluids. Results show that on average Rn activity,  $\text{CO}_2$  concentration,  $\phi\text{CO}_2$  and  $\phi\text{CH}_4$  are lower than those measured in cultivated areas of the Modena province, whereas  $\text{CH}_4$  concentrations are higher.

The distribution of trace elements such as  $^{222}\text{Rn}$ , He, and  $\text{H}_2$  were studied in order to identify potential faults and/or fractures related to preferential migration pathways and the possible interactions between reservoir and surface. Anomalous  $\phi\text{CO}_2$  and  $\phi\text{CH}_4$ , Rn activities and  $\text{CO}_2$ ,  $\text{CH}_4$ , He,  $\text{H}_2$  concentrations, observed in the two regions at the edge of the NMV (NE and SW), indicate the presence of high permeability areas. Here tectonic structures controlling the collapse of the caldera are interpreted to be the preferential leakage pathways for the migrating gas. Other anomalies ( $\phi\text{CO}_2$ ) are located along a morphological slope in the

1 central part of the crater suggesting the observed morphological escarpment has a tectonic control for gas  
2 migration.

3 Estimated CH<sub>4</sub> micro and macro-seepage values are lower than those measured during previous surveys in  
4 the NMV and in other areas of Po Plain. This suggests that the NMV is in a relative quiescent activity period  
5 where lower gas emissions from active gryphons are associated with a wider spatial distribution.  
6

7  
8 The extruded gas is methane-dominated with minor amounts of nitrogen, oxygen, carbon dioxide, and  
9 ethane. Isotopic analyses highlight the thermogenic origin of emitted methane, in agreement with previous  
10 literature. Noble-gas elemental and isotopic signatures constrain the crustal origin of these emissions.  
11

12 Soil gas monitoring allowed to constrain the relationship between geochemistry and tectonics, and permitted  
13 the identification of areas with high permeability where new mud emissions occurred after to this survey.  
14

15 This survey highlights that the newly born active site in the NE of the crater zone is the most active.  
16

17 Potentially other eruptive phenomena could be expected in the future following the same NE trend.  
18  
19  
20  
21  
22

## 23 **Acknowledgements**

24  
25 A.M. was financially supported by the European Research Council under the European Union's Seventh  
26 Framework Programme Grant agreement n 308126 (LUSI LAB project, PI A. Mazzini). We acknowledge  
27 the support from the Research Council of Norway through its Centers of Excellence funding scheme, Project  
28 Number 223272 (CEED). Field surveys were supported by Fiorano Municipality in collaboration with  
29 UNIMORE (Accordo di ricerca tra il Comune di Fiorano Modenese e il Dipartimento di Scienze Chimiche e  
30 Geologiche dell'Università di Modena e Reggio Emilia)  
31  
32  
33  
34  
35  
36  
37  
38  
39  
40  
41

## 42 **References**

43  
44 Aeschbach-Hertig, W., Peeters, F., Beyerle, U., Kipfer, R., 1999. Interpretation of dissolved atmospheric  
45 noble gases in natural waters. *Water Resour. Res.* 35(9), 2779–2792.  
46

47  
48 Aeschbach-Hertig, W., and Solomon, D.K., 2013. Noble Gas Thermometry in Groundwater Hydrology. In:  
49 Burnard, P. (Ed.), *The Noble Gases as Geochemical Tracers. Advances in Isotope Geochemistry*. Berlin,  
50 Heidelberg: Springer, pp. 81–122.  
51

52  
53  
54 Accaino, F., Bratus, A., Conti, S., Fontana, D., Tinivella, U., 2007. Fluid seepage in mud volcanoes of the  
55 northern Apennines: An integrated geophysical and geological study. *Journal of Applied Geophysics* 63, 90–  
56 101.  
57  
58  
59  
60  
61  
62  
63  
64  
65

- 1 Ballentine, C.J., and Hall, C.M., 1999. Determining paleotemperature and other variables by using an error-  
2 weighted, nonlinear inversion of noble gas concentrations in water. *Geochim. Cosmochim. Acta* 63(16),  
3 2315–2336.  
4
- 5 Barbieri, G., 1947. Nuove osservazioni sulle salse emiliane. *Riv. Geogr. It.*, 54, 172-185.  
6
- 7  
8 Baubron, J.C., Rigo, A., Toutain, J.P., 2002. Soil gas profiles as a tool to characterise active tectonic areas:  
9 the Jaut Pass example(Pyrenees, France). *Earth Planet. Sci. Lett.* 196, 69–81.  
10
- 11  
12 Beaubien, S.E., Ciotoli, G., Lombardi, S., 2003. Carbon dioxide and radon gas hazard in the Alban Hills area  
13 (central Italy). *J. Volcanol. Geotherm. Res.* 123, 63–80.  
14
- 15  
16 Bertacchini, M., Giusti, C., Marchetti, M., Panizza, M. & Pellegrini, M., (eds.) 1999. I beni geologici della  
17 Provincia di Modena. Artioli Ed., Modena, 104 pp.  
18
- 19  
20  
21 Bertrami, R., Ceccarelli, A. & Lombardi, S., 1984. L'elio dei gas del suolo nella prospezione geotermica.  
22 *Rend. Soc. Ital. Mineral. Petrogr.*, 39, 331-342.  
23
- 24  
25 Beyerle, U., Aeschbach-Hertig, W., Imboden, D.M., Baur, H., Graf, T., Kipfer, R., 2000. A mass  
26 spectrometric system for the analysis of noble gases and tritium from water samples. *Environ. Sci. Technol.*  
27 34, 2042–2050.  
28
- 29  
30  
31 Biasutti, R., 1907. Le salse dell'Appennino settentrionale. *Mem. Geogr.* II, pp. 101-255.  
32
- 33  
34 Benedetti, L.C., Tapponnier, P., Gaudemer, Y., Manighetti, I., Van der Woerd, J., 2003. Geomorphic  
35 evidence for an emergent active thrust along the edge of the Po Plain: The Broni-Stradella fault. *J. Geophys.*  
36 *Res.*, v. 108, 2238, doi: 10.1029/2001JB001546.  
37
- 38  
39 Bergfeld, D., Goff, F., and Janik, C.J., 2001. Elevated carbon dioxide flux at the Dixie Valley geothermal  
40 field, Nevada: Relations between surface phenomena and the geothermal reservoir. *Chem. Geol.*, 177(1–2),  
41 43–66.  
42
- 43  
44  
45 Bonini, M., 2007. Interrelations of mud volcanism, fluid venting, and thrust-anticline folding: Examples  
46 from the external northern Apennines (Emilia-Romagna, Italy). *J. Geophys. Res.*, 112, B08413,  
47 doi:10.1029/2006JB004859.  
48
- 49  
50  
51 Bonini, M., 2008. Elliptical mud volcano caldera as stress indicator in an active compressional setting  
52 (Nirano, Pede-Apennine margin, northern Italy). *Geology*, 36, 131-134.  
53
- 54  
55  
56 Bonini, M., 2009. Mud volcano eruptions and earthquakes in the Northern Apennines and Sicily, Italy.  
57 *Tectonophysics*, 474, 723–735.  
58
- 59  
60  
61  
62  
63  
64  
65

1 Bonini, M., 2012. Mud volcanoes: Indicators of stress orientation and tectonic controls. *Earth-Science*  
2 *Reviews* 115, 121-152.

3  
4 Brennwald, M.S., Hofer, M., Peeters, F., Aeschbach-Hertig, W., Strassmann, K., Kipfer, R., Imboden, D.M.,  
5 2003. Analysis of dissolved noble gases in the pore water of lacustrine sediments. *Limnol. Oceanogr.*  
6 *Methods* 1, 51–62.

7  
8  
9  
10 Brennwald, M.S., Vogel, N., Scheidegger, Y., Tomonaga, Y., Livingstone, D.M., Kipfer, R., 2013. Noble  
11 gases as environmental tracers in sediment porewaters and in stalagmite fluid inclusions. In: Burnard, P.  
12 (Ed.), *The Noble Gases as Geochemical Tracers. Advances in Isotope Geochemistry*. Berlin, Heidelberg:  
13 Springer, pp. 123–153.

14  
15  
16  
17 Capozzi R., Picotti V., 2002. Fluid migration and origin of a mud volcano in the Northern Apennines (Italy):  
18 The role of deeply rooted normal faults. *Terra Nova* 14:363–370

19  
20  
21 Capozzi R., Menato V., Rabbi E., 1994. Manifestazioni superficiali di fluidi ed evoluzione tettonica recente  
22 del margine Appenninico Emiliano-Romagnolo: indagine preliminare. *Atti Ticinensi Scienze Terra* 1:247–  
23 254.

24  
25  
26  
27 Castaldini, D., Chiriach. C., Ilies. D.C. & Barozzini. E.. 2003- Documenti digitali per la conoscenza integrata  
28 dei Geositi: l'esempio della Riserva Naturale delle Salse di Nirano. In: S. Piacente & G. Poli (eds.). *La*  
29 *Memoria della Terra. Regione Emilia Romagna. Ed. L'inchiostro blu*. Bologna, 121-127.

30  
31  
32  
33 Castaldini, D., Valdati, J., Ilies, D.C., Chiriach, C., Bertogna, I., 2005. Geo-Tourist map of the natural Reserve  
34 of salse di Nirano (Modena Apennines, Northern Italy). *Il Quaternario*, 18, 245-255.

35  
36  
37  
38 Castaldini, D., Conti S., Conventi M., Dallai D., Del Prete C., Fazzini M., Fontana D., Gorgoni C., Ghinoi  
39 A., Russo A., Sala L., Serventi P., Verri D., and Barbieri M., 2007. *Le Salse di Nirano*. CD ROM.  
40 *Enciclopedia Multimediale*. Comune di Fiorano Modenese.

41  
42  
43  
44 Castaldini, D., Conventi, M., Coratza, P., & Liberatoscioli, E., 2011. La “Nuova” Carta Turistico -  
45 Ambientale della Riserva Naturale Regionale delle Salse di Nirano (Appennino Modenese, Italia  
46 Settentrionale). *Bollettino A.I.C.* nr.143/2011, I275-289.

47  
48  
49  
50 Chiodini, G., and Frondini, F. 2001. Carbon dioxide degassing from the Albani Hills volcanic region, Central  
51 Italy. *Chemical Geology*, 177, 67–83.

52  
53  
54  
55 Chiodini, G., Cioni, R., Guidi, M., Raco, B., Marini, L., 1998. Soil CO<sub>2</sub> flux measurements in volcanic and  
56 geothermal areas. *Appl. Geochem.* 13, 543–552.

- 1 Ciotoli, G., Lombardi, S., Morandi, S., Zarlenga, F., 2005. A multidisciplinary statistical approach to study  
2 the relationships between helium leakage and neo-tectonic activity in a gas province. The Vasto Basin,  
3 Abruzzo-Molise (central Italy). *Am. Assoc. Petrol. Geol. Bull.* 88, 355–372.  
4
- 5 Ciotoli, G., Lombardi, S., Annunziatellis, A., 2007. Geostatistical analysis of soil gas data in a high seismic  
6 intermontane basin: Fucino Plain, central Italy. *J. Geophys. Res.* 112, B05407.  
7 <http://dx.doi.org/10.1029/2005JB004044>.  
8  
9
- 10 Ciotoli, G., Sciarra A., Ruggiero, L., Annunziatellis, A., Bigi, S., 2016. Soil gas geochemical behaviour  
11 across buried and exposed faults during the 24 August 2016 central Italy earthquake. *Ann- of Geoph.* 59,  
12 Fast Track 5, doi:10.4401/ag-7242.  
13  
14  
15
- 16 Cipriani, A., Lugli, F., Martinelli, G., Sciarra, A., 2017. Analisi isotopiche ( $^{87}\text{Sr}/^{86}\text{Sr}$ ,  $\delta^{18}\text{O}$ ,  $\delta\text{D}$  e trizio) delle  
17 Salse di Nirano. *Suppl. Atti Soc. Nat. Mat. di Modena*, 148, 155-165. ISSN 0365 - 7027.  
18  
19  
20
- 21 Coppi, F., 1875. Brevi note sulle Salse Modenesi. *Bollettino del R. Comitato Geologico*, 7-8, 1-7.  
22  
23
- 24 Etiopie, G., and Lombardi, S., 1995. Evidence for radon transport by carrier gas through faulted clays in Italy.  
25 *J. Radioanalyt. Nucl. Chem.* 193 (2), 291–300.  
26  
27
- 28 Etiopie, G., 2004. New directions: GEM – Geologic Emissions of Methane, the missing source in the  
29 atmospheric methane budget. *Atmospheric Environment*, 38 (19), 3099-3100, DOI:  
30 [10.1016/j.atmosenv.2004.04.002](http://dx.doi.org/10.1016/j.atmosenv.2004.04.002).  
31  
32  
33
- 34 Etiopie, G., Martinelli, G., Caracausi, A., Italiano, F., 2007. Methane seeps and mud volcanoes in Italy: gas  
35 origin, fractionation and emission to the atmosphere. *Geophys. Res. Lett.* 34, L14303.  
36 <http://dx.doi.org/10.1029/2007GL030341>  
37  
38  
39
- 40 Etiopie, G., Feyzullayev, A., Baciù, C.L., 2009. Terrestrial methane seeps and mud volcanoes: a global  
41 perspective of gas origin. *Mar. Petr. Geol.* 26(3), 333–344.  
42  
43
- 44 Etiopie, G., 2015. Natural Gas Seepage. *The Earth's Hydrocarbon Degassing*. Springer International  
45 Publishing, Switzerland: p. 199 <http://dx.doi.org/10.1007/978-3-319-14601-0> (ISBN 978-3-319-14601-0  
46 (eBook)).  
47  
48  
49
- 50 Ferrari, C., and Vianello, G., 1985. Le Salse dell'Emilia-Romagna. Regione Emilia-Romagna, Collana  
51 Assessorato Ambiente, 116-118.  
52  
53
- 54 Gasperi, G., Cremaschi, M., Mantovani Uguzzoni, M.P., Cardarelli, A., Cattani, M., & Labate, D., 1989.  
55 Evoluzione Plio-Quaternaria del margine appenninico modenese e dell'antistante pianura. Note illustrative  
56 alla Carta Geologica. *Mem. Soc. Geol. It.*, 39, 431 pp.  
57  
58  
59  
60  
61  
62  
63  
64  
65

- 1 Gorgoni, C., 2003. Le salse di Nirano e le altre salse emiliane - I segreti di un fenomeno tra mito e realtà -  
2 Comune di Fiorano Modenese. Tip. ABC, Sesto Fiorentino (Firenze), 128 pp.  
3
- 4 Gorgoni, C., Bonori, O., Lombardi, S., Martinelli, G., and Sighinolfi, G.P., 1988. Radon and helium  
5 anomalies in mud volcanoes from northern Apennines (Italy) –a tool for earthquake prediction. *Geochemical*  
6 *Journal*, 22, 265-273.  
7  
8  
9
- 10 Grassa, F., Capasso, G., Favara, R., Inguaggiato, S., Faber, E. and Valenza, M., 2004. Molecular and isotopic  
11 composition of free hydrocarbon gases from Sicily, Italy. *Geophysical Research Letters* 31, L06607.  
12 doi:10.1029/2003GL019362.  
13  
14  
15
- 16 Heller, C., Blumenberg, M., Kokoschka, S., Wrede, C., Hoppert, M., Taviani, M., and Reitner, J., 2011.  
17 Geomicrobiology of Fluid Venting Structures at the Salse di Nirano Mud Volcano Area in the Northern  
18 Apennines (Italy). In J. Reitner et al., *Advances in Stromatolite Geobiology, Lecture Notes in Earth Sciences*  
19 131, , pp.209-220. DOI 10.1007/978-3-642-10415-2\_14  
20  
21  
22
- 23 Heller, C., Blumenberg, M., Hoppert, M., Taviani, M., Reitner, J., 2012. Terrestrial mud volcanoes of the  
24 Salse di Nirano (Italy) as a window into deeply buried organic –rich shales of Plio-Pleistocene age.  
25 *Sedimentary Geology*, 263, 202-209. DOI: 10.1016/j.sedgeo.2011.05.004.  
26  
27  
28
- 29 Henry, P., Le Pichon, X.L., Lallemand, S., Foucher, J.-P., Westbrook, G., Hobart, M., 1990, Mud volcano  
30 field seaward of the Barbados Accretionary Complex: A deep-towed scan sonar survey: *J. Geophys. Res.* 95,  
31 p. 8917–8929  
32  
33  
34
- 35 Hermansson, H.P., Akerblom, G., Chyssler, J., Linden, A., 1991. Geogas, a carrier or a tracer? SKN report  
36 51.  
37  
38
- 39 Hinkle, M., 1994. Environmental conditions affecting concentrations of He, CO<sub>2</sub>, O<sub>2</sub> and N<sub>2</sub> in soil gases.  
40 *Appl. Geochem.* 9, 53–63.  
41  
42  
43
- 44 Hutchinson, G.L., Livingston, G.P., Healy, R.W., Striegl, R.G., 2000. Chamber measurement of surface–  
45 atmosphere trace gas exchange: numerical evaluation of dependence on soil, interfacial layer and source/sink  
46 properties. *J. Geophys. Res.* 105, 8865–8875.  
47  
48
- 49 Kopf A. (2002) - Significance of mud-volcanism. *Review of Geophysics*, 40 (2), 1-52.  
50  
51
- 52 Inguaggiato, S., and Rizzo, A.L., 2004. Dissolved helium isotope ratios in ground-waters: A new technique  
53 based on gas-water re-equilibration and its application to Stromboli volcanic system. *Appl. Geochem.* 19(5),  
54 665-673, DOI: 10.1016/j.apgeochem.2003.10.009.  
55  
56  
57  
58  
59  
60  
61  
62  
63  
64  
65



- 1  
2  
3  
4  
5  
6  
7  
8  
9  
10  
11  
12  
13  
14  
15  
16  
17  
18  
19  
20  
21  
22  
23  
24  
25  
26  
27  
28  
29  
30  
31  
32  
33  
34  
35  
36  
37  
38  
39  
40  
41  
42  
43  
44  
45  
46  
47  
48  
49  
50  
51  
52  
53  
54  
55  
56  
57  
58  
59  
60  
61  
62  
63  
64  
65
- Lee, J. Y., Marti, K., Severinghaus, J. P., Kawamura, K., Yoo, H. S., Lee, J. B., Kim, J. S., 2006. A redetermination of the isotopic abundances of atmospheric Ar. *Geochim. Cosmochim. Acta* 70(17):4507–4512.
- Lupi, M., Suski Ricci, B., Kenkel, J., Ricci, T., Fuchs, F., Miller, S.A. & Kemna, A., 2016. Subsurface fluid distribution and possible seismic precursory signal at the Salse di Nirano mud volcanic field, Italy. *Geophys. J. Int.*, p. 907-917, doi:10.1093/gji/ggv454.
- Madonia, P., Grassa, F., Cangemi, M., and Musumeci, C., 2011, Geomorphological and geochemical characterization of the 11 August 2008 mud volcano eruption at S. Barbara village (Sicily, Italy) and its possible relationship with seismic activity: *Natural Hazards and Earth System Sciences*, v. 11, p. 1545-1557.
- Mamyrin, B.A., and Tolstikhin, I.N., 1984. *Helium Isotopes in Nature*. Elsevier, Amsterdam.
- Manga, M., and Bonini, M., 2012. Large historical eruptions at subaerial mud volcanoes, Italy. *Nat. Hazards Earth Syst. Sci.*, 12(11), 3377–3386, doi:10.5194/nhess-12-3377-2012.
- Martinelli, G., 1999. Mud volcanoes of Italy: a review. *Giornale di Geologia*, ser. 3,61, 107-113.
- Martinelli, G., and Rabbi, E., 1998. The Nirano mud volcanoes. In: Curzi P.V., Judd A.G. (eds) *Abstracts and Guide Book, V<sup>th</sup> International Conference on Gas in Marine Sediments*, Bologna, Italy; September 1998. Grafiche A & B, Bologna, pp 202-206
- Martinelli, G., and Judd, A., 2004. Mud volcanoes of Italy. *Geological Journal* 39, 49–61.
- Mazzini, A., Svensen, H., Planke, S., Guliyev, I., Akhmanov, G.G., Fallik, T., and Banks, D., 2009. When mud volcanoes sleep: insight from seep geochemistry at the Dashgil mud volcano, Azerbaijan. *Mar. Petrol. Geol.* 26, 1704-1715. doi:10.1016/j.marpetgeo.2008.11.003.
- Mazzini, A., and Etiope, G., 2017, Mud volcanism: An updated review: *Earth-Science Reviews*, v. 168, p. 81–112.
- Minissale, A., Magro, G., Martinelli, G., Vaselli, O., Tassi, G.F., 2000. Fluid geochemical transect in the Northern Apennines (central-northern Italy): fluid genesis and migration and tectonic implications. *Tectonophysics* 319, 199–222.
- Mucchi, A.M., 1966. Il fenomeno delle salse e le manifestazioni del Modenese. *Atti Soc. Nat. Mat. Modena*, 97, 1-31.
- Mucchi, A.M., 1968. Le salse del Modenese e del Reggiano. *L'Universo*, 48 (3), 421-436.
- Pallasser, R.J., 2000. Recognising biodegradation in gas/oil accumulations through the  $\delta^{13}\text{C}$  compositions of gas components. *Org. Geochem.* 31, 1363–1373.

- 1 Pantanelli, D., and Santi, V., 1896. L'Appennino Modenese. Ed. Cappelli, Rocca San Casciano, Ristampa  
2 1996, Ed. Iaccheri, Pavullo nel Frignano.
- 3
- 4 Pellegrini, M., Brazzorotto, C., Forti, P., Francavilla, F., & Rabbi, E., 1982. Idrogeologia del margine pede-  
5 appenninico emiliano romagnolo, In: G. Cremonini & F. Ricci Lucchi (eds.) –Guida alla geologia del  
6 margine appenninico-padano. Guida Geol. Reg., Soc. Geol. It., Bologna, 183-189.
- 7
- 8
- 9
- 10 Pieri, M., and Groppi, G., 1981. Subsurface Geological Structure of the Po Plain. Italy. Pubbl. 414, Progetto  
11 Finalizzato Geodinamica, C.N.R.
- 12
- 13
- 14 Quattrocchi, F., Pizzi, A., Gori, S., Boncio, P., Voltattorni, N., Sciarra, A., 2012. The contribution of fluid  
15 geochemistry to define the structural pattern of the 2009 L'Aquila seismic source. *Int. J. Geosc.* 131, 448–  
16 458. <http://dx.doi.org/10.3301/IJG.2012.31> (ISSN: 2038–1727).
- 17
- 18
- 19
- 20 Saunois, M., Bousquet, P., Poulter, B., Peregon, A., Ciais, P., Canadell, J.G., Dlugokecky, E.J., Etiope, G.,  
21 Bastviken, D., Houweling, S., Janssens-Maenhout, G., et al., 2016. The Global Methane Budget: 2000-2012.  
22 *Earth Syst. Sci. Data Discuss.*, doi:10.5194/essd-2016-25.
- 23
- 24
- 25
- 26 Schoell, M., 1980. The hydrogen and carbon isotopic composition of methane from natural gases of various  
27 origins. *Geochim. Et Cosmochim. Acta* 44, 649–661.
- 28
- 29
- 30 Sciarra, A., Cinti, D., Pizzino, L., Procesi, M., Voltattorni, N., Mecozzi, S., Quattrocchi, F., 2013.  
31 Geochemistry of shallow aquifers and soil gas surveys in a feasibility study at the Rivara natural gas storage  
32 site (Po Plain, Northern Italy). *App. Geoch.*, 34, 3-22. <http://dx.doi.org/10.1016/j.apgeochem.2012.11.008>
- 33
- 34
- 35
- 36 Sciarra, A., Cantucci, B., Castaldini, D., Procesi, M., Conventi, M., 2015a. Between history, work and  
37 passion: medieval castle, mud volcanoes and Ferrari. *Geol. F. Trips* 7 (n.1.1), 42pp. DOI  
38 10.3301/GFT.2015.01; ISSN 2038-4947.
- 39
- 40 Sciarra, A., Fascetti, A., Moretti, A., Cantucci, B., Pizzino, L., Lombardi, S., Guerra, I., 2015b. Geochemical  
41 and radiometric profiles through an active fault in the Sila Massif (Calabria, Italy). *J. Geochem. Explor.* 148,  
42 128-137.
- 43
- 44
- 45
- 46 Sciarra, A., Cantucci, B., Coltorti, M., 2017. Learning from soil gas change and isotopic signatures during  
47 the 2012 Emilia seismic sequence. *Scientific Reports*, 7, 14187, doi: 10.1038/s41598-017-14500-y.
- 48
- 49
- 50 Sciarra, A., Mazzini, A., Inguaggiato, S., Vita, F., Lupi, A., and Hadi, S., 2018. Radon and carbon gas  
51 anomalies along the Watukosek fault system and Lusi mud eruption, Indonesia: *Marine & Petroleum*  
52 *Geology* 90, 77-90. <https://doi.org/10.1016/j.marpetgeo.2017.09.031>.
- 53
- 54
- 55
- 56 Segovia, N., Seidel, J.L., Monnin, M., 1987. Variations of radon in soils induced by external factors. *J.*  
57 *Radioanal. Nucl. Chem. Lett.* 119, 199–209.
- 58
- 59
- 60
- 61
- 62
- 63
- 64
- 65

- 1 Sinclair, A.J., 1974. Selection of threshold values in geochemical data using probability graphs. *J. Geochem.*  
2 *Explor.* 3, 129–149.
- 3  
4 Sinclair, A.J., 1991. A fundamental approach to threshold estimation in exploration geochemistry:  
5 probability plots revisited. *J. Geochem. Explor.* 41, 1–22.
- 6  
7  
8 Stoppani, A., 1873. *Il Bel Paese*. Milano, 651 pp.
- 9  
10 Tassi, F., Bonini, M., Montegrossi, G., Capecchiacci, F., Capaccioni, B., Vaselli, O., 2012. Origin of  
11 hydrocarbons in gases from mud volcanoes and CH<sub>4</sub>-rich emissions. *Chem. Geol.* 294 (295), 113–126.
- 12  
13  
14 Tomonaga, Y., Brennwald, M.S., Kipfer, R., 2011. An improved method for the analysis of dissolved noble  
15 gases in the pore water of unconsolidated sediments. *Limnol. Oceanogr. Methods* 9, 42–49.  
16 doi:10.4319/lom.2011.9.42
- 17  
18  
19 Tomonaga, Y., Brennwald, M.S., Kipfer, R., 2013. Using helium and other noble gases in ocean sediments to  
20 characterize active methane seepage off the coast of New Zealand. *Mar. Geol.* 344, 34–40,  
21 doi:10.1016/j.margeo.2013.07.010.
- 22  
23  
24 Tomonaga, Y., Brennwald, M.S., Meydan, A.F., Kipfer, R., 2014. Noble gases in the sediments of Lake Van  
25 - Solute transport and palaeo-environmental reconstruction. *Quat. Sci. Rev.* 104, 117–126,  
26 doi:10.1016/j.quascirev.2014.09.005.
- 27  
28  
29 Tomonaga, Y., Brennwald, M.S., Kipfer, R., 2015. Attenuation of noble-gas transport in laminated  
30 sediments of the Stockholm Archipelago. *Limnol. Oceanogr.* 60(2), 497–511, doi:10.1002/lno.10045.
- 31  
32  
33 Tyroller, L., Tomonaga, Y., Brennwald, M.S., Ndayisaba, C., Naeher, S., Schubert, C., North, R.P., Kipfer,  
34 R., 2016. Improved method for the quantification of methane concentrations in unconsolidated lake  
35 sediments. *Environ. Sci. Technol.* 50(13), 7047–7055, doi:10.1021/acs.est.5b05292.
- 36  
37  
38 Valente, E., Ascione, A., Ciotoli, G., Cozzolino, M., Porfido, S., Sciarra, A., 2018. Do moderate magnitude  
39 earthquakes generate seismically induced ground effects? The case study of the Mw = 5.16, 29th December  
40 2013 Matese earthquake (southern Apennines, Italy). *Int. J. Earth Sci. (Geol. Rundsch.)* 107, 517-537.  
41 <https://doi.org/10.1007/s00531-017-1506-5>.
- 42  
43  
44 Wang, W.C., Zhang, L.Y., Liu, W.H., Kang, Y., & Ren, J.H., 2005. Effects of biodegradation on the carbon  
45 isotopic composition of natural gas — a case study in the Bamianhe oil field of the Jiyang Depression,  
46 Eastern China. *Geochemical Journal*, 39, 301–309.
- 47  
48  
49  
50  
51  
52  
53  
54  
55  
56  
57  
58  
59  
60  
61  
62  
63  
64  
65

Figure 1

[Click here to download high resolution image](#)

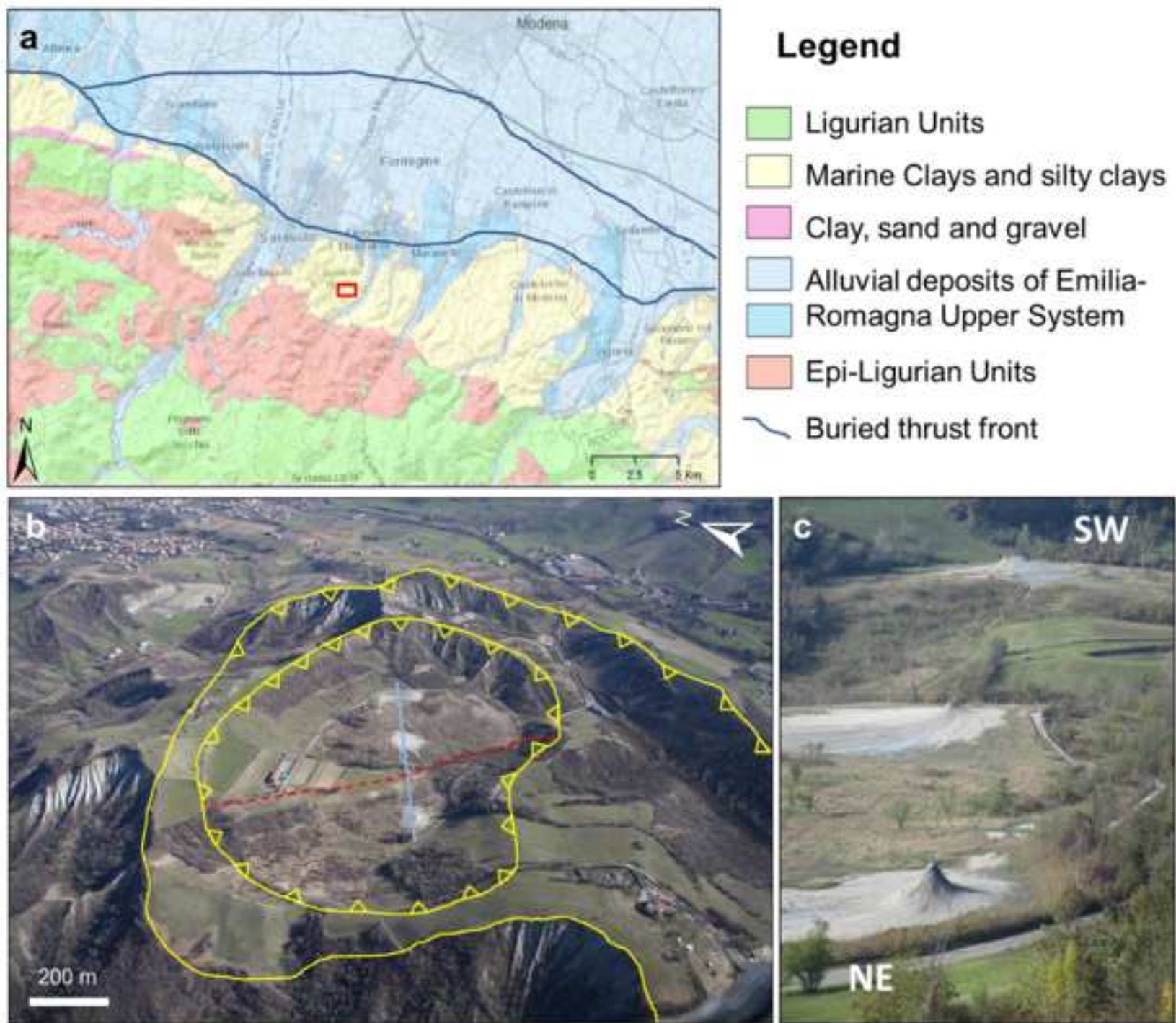


Figure 2  
[Click here to download high resolution image](#)

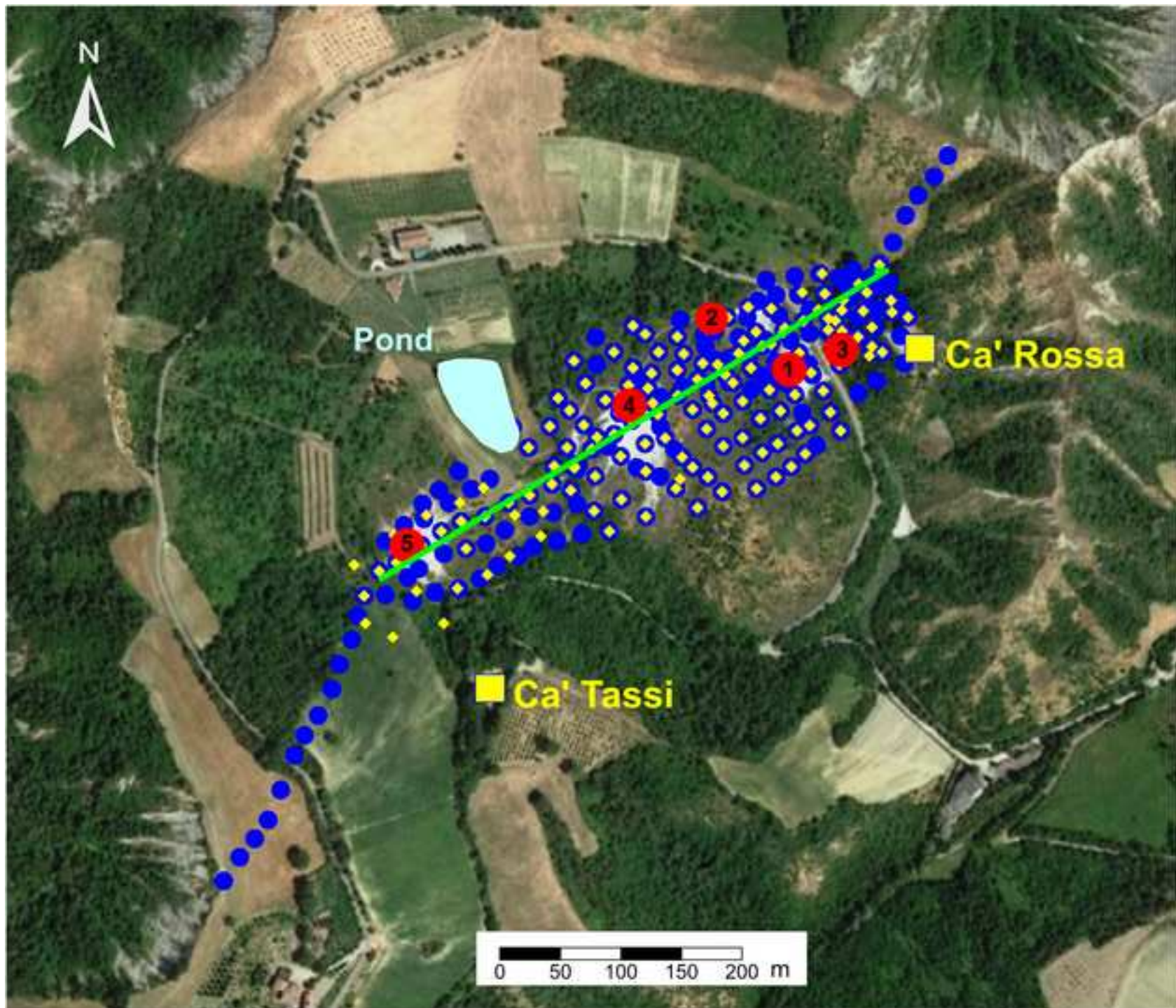


Figure 3  
[Click here to download high resolution image](#)

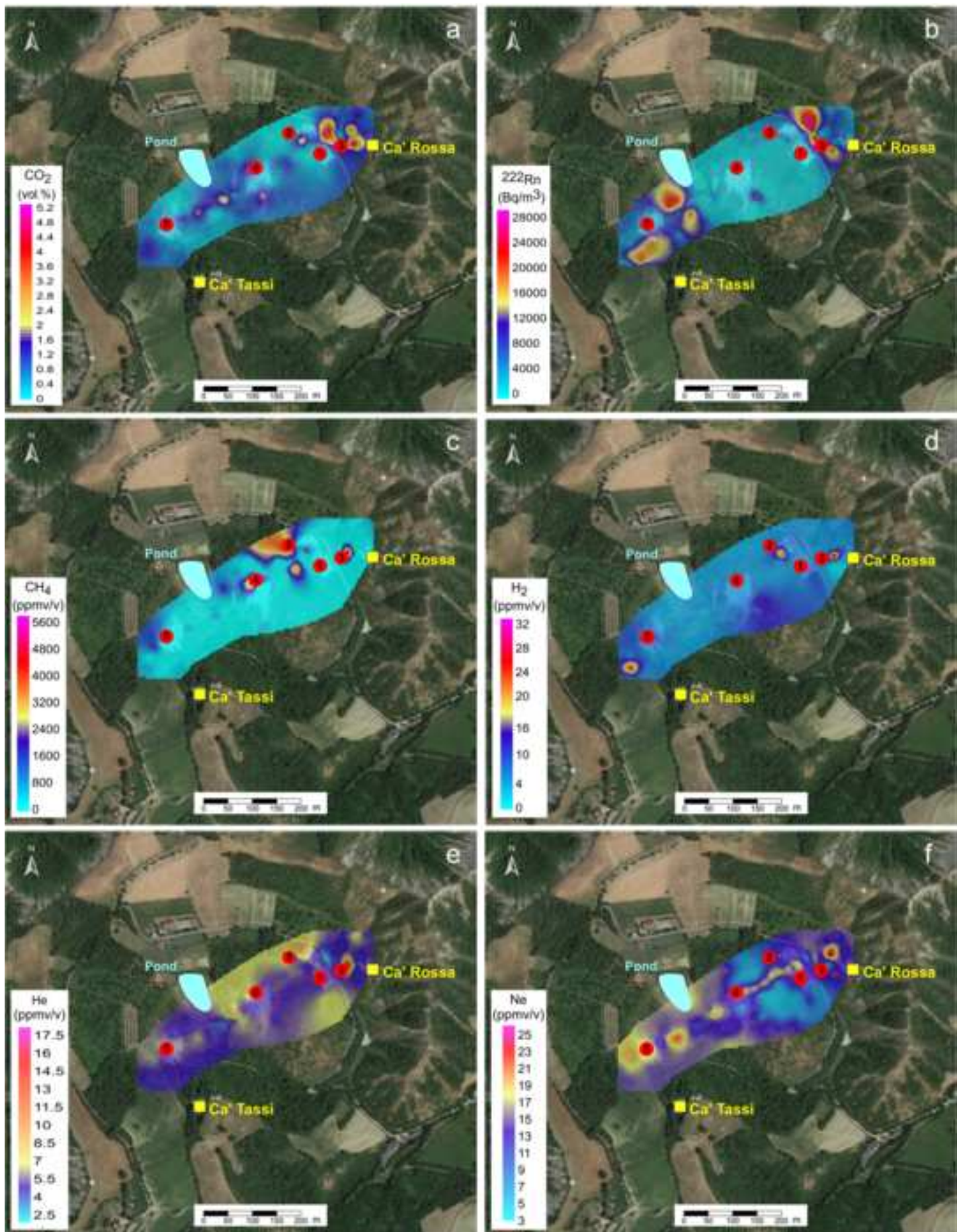


Figure 4  
[Click here to download high resolution image](#)

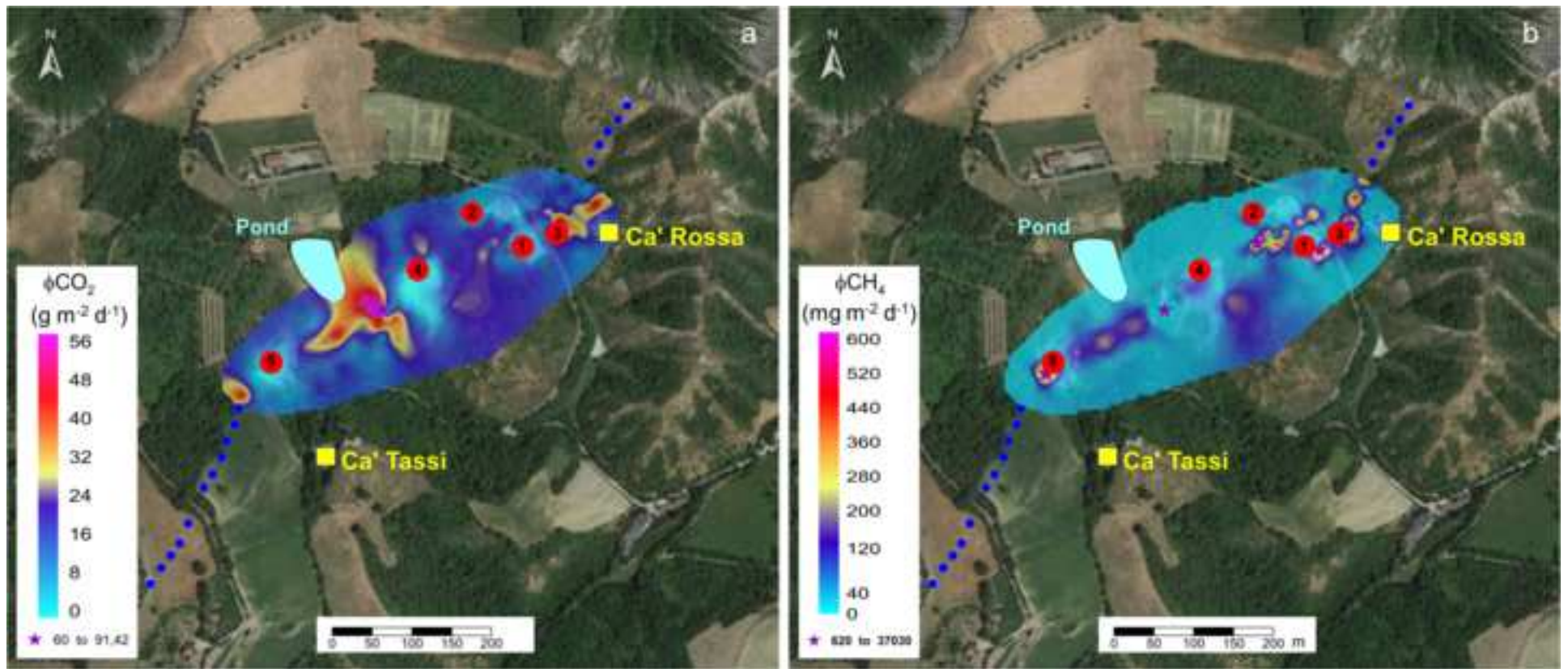


Figure 5  
[Click here to download high resolution image](#)





Figure 6  
[Click here to download high resolution image](#)

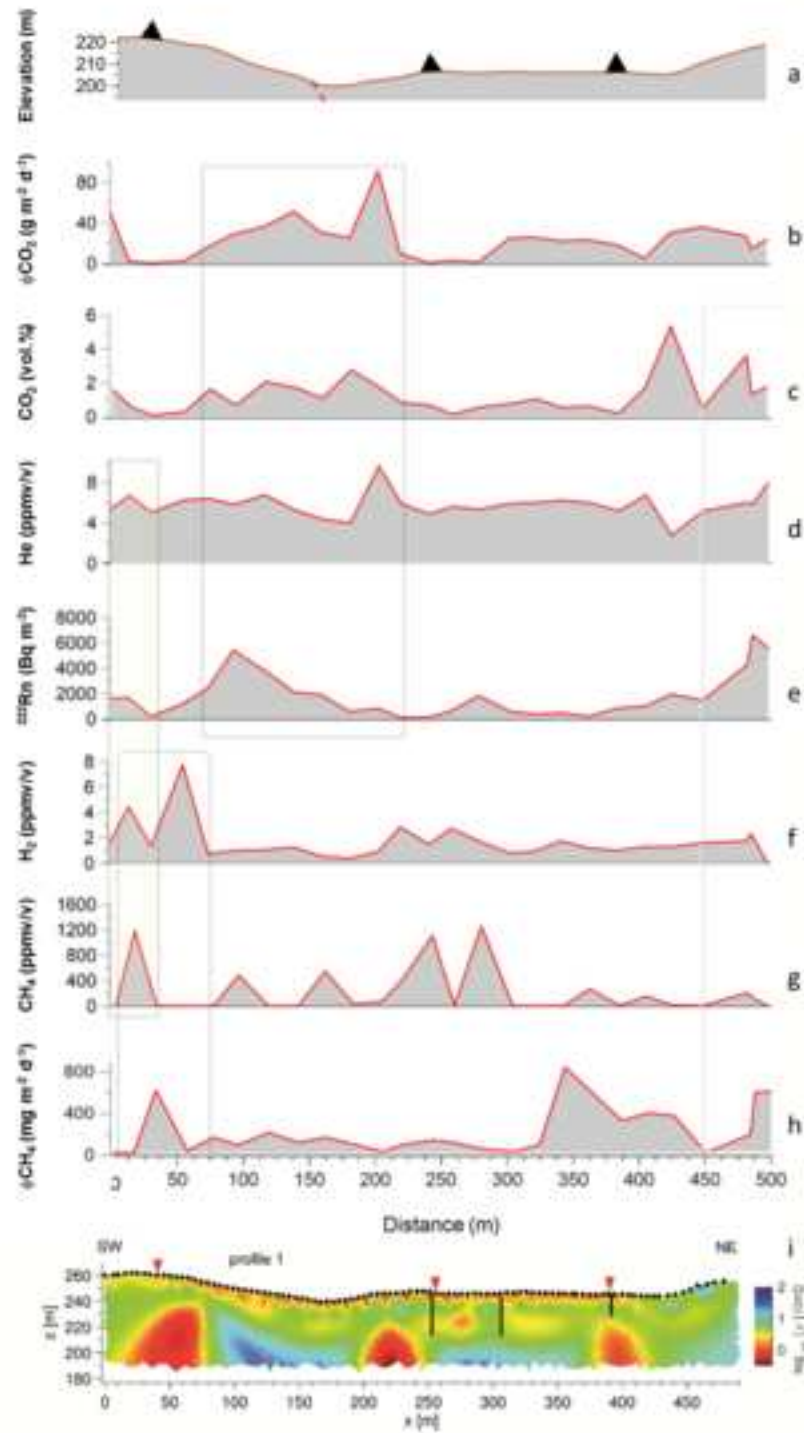


Figure 7  
[Click here to download high resolution image](#)

